Thermal Management Of The CBM-FAIR's Silicon Tracking System (STS) – Concept And Demonstrator –

Kshitij Agarwal

/ʂɪ.t̪ɪd͡ʒ əg.rᵊ.vɑːl/

Eberhard-Karls-Universität Tübingen (DE)

– For the CBM Collaboration –

Forum on Tracking Detector Mechanics

Eberhard Karls Universität Tübingen, May 31 – June 02, 2023

EBERHARD KARLS UNIVERSITÄT TÜBINGEN

MATHEMATISCH-NATURWISSENSCHAFTLICHE FAKULTÄT
Physikalisches Institut

GSI

CBM

FAIR

Introduction

FAIR CONTRUCTION STATUS (APRIL 2023)

FAIR Contruction Status (April 2023)

- Interior work on SIS-100 tunnel ongoing - SIS100 ready for commissioning w/ beams 2028
- CBM Building's construction is on schedule and with 'heavy installations' like internal crane commissioned
- CBM ready for beam in 2027-28, ~12 months contingency for CBM global commissioning
- Updates on construction available at: GSI Webpage |CBM Webpage | YouTube | …

Compressed Baryonic Matter (CBM) Experiment

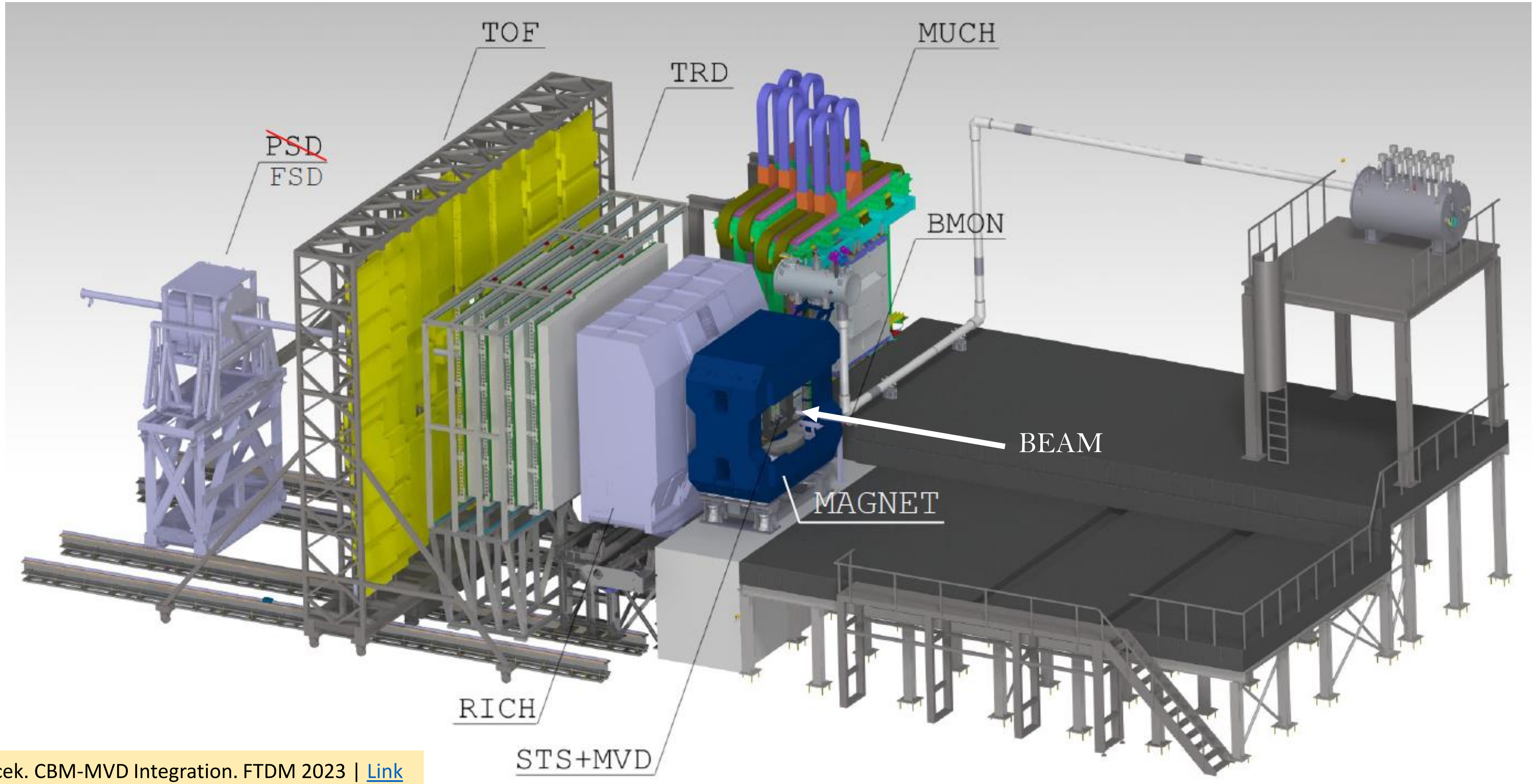

F. Matejcek. CBM-MVD Integration. FTDM 2023 | Link

(Thermal) Introduction To CBM-STS

STS-Module: Silicon Sensors + Shielded Microcables + FEE-Boards (FEBs)

- Double-sided silicon microstrip silicon sensors connected to the front-end electronics (FEEs) via ultra-light shielded microcables
- End-of-Lifetime (EOL) radiation up to 10^{14} n_{eq}/cm^2 (1 MeV eq.)
- FEEs outside the physics aperture dissipating approx. 25W per module

STS Stations (Tracking Layers, including peripherally located electronics & services)

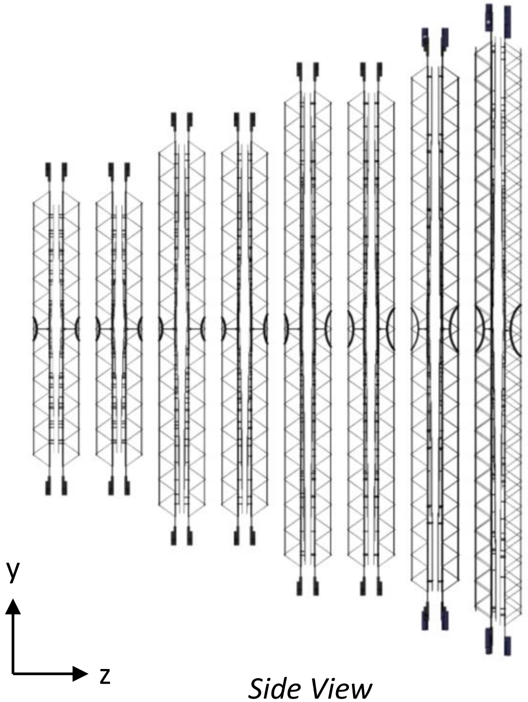

Side View

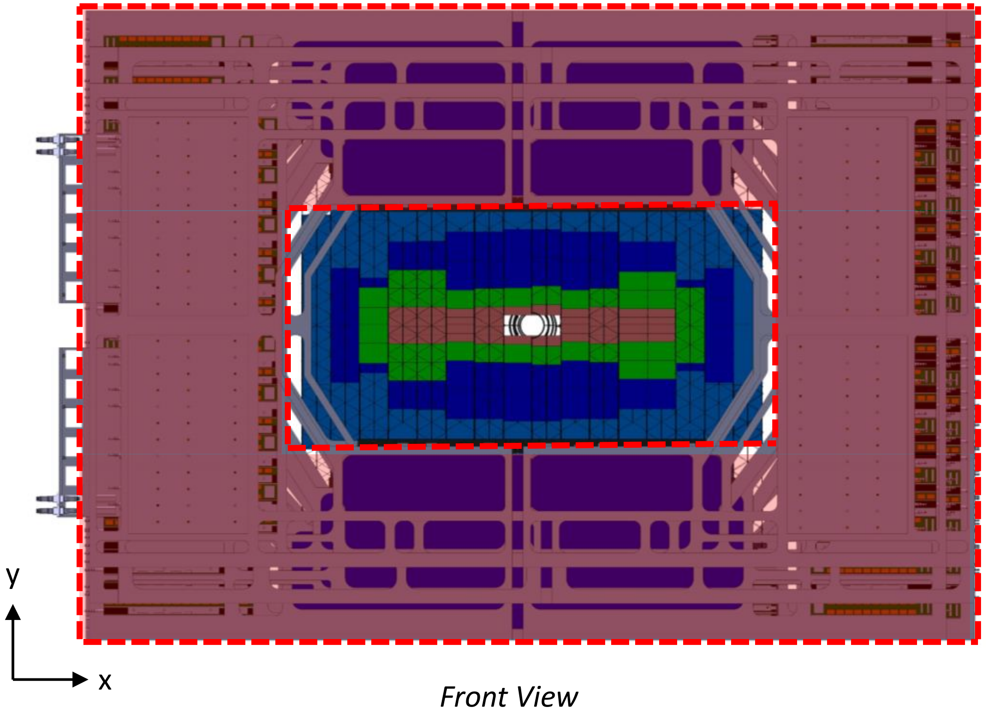

Front View

- 8 tracking stations, 0.3 – 1.0 m downstream target
- ≈ 4 m^2 area, 876 modules, 1.8 M channels
- Sensors mounted to carbon-fibre ladders
- Material budget per station: ≈ 0.3% – 2% X_0
- Total FEE power dissipation of approx. 40 kW
- Located inside an aluminium-cladded CF-Foam thermal and electromagnetic enclosure

M. Teklishyn. CBM-STS Integration. FTDM 2022 | Link
L.M. Collazo Sánchez. STS-FEE Thermal Aspects. FTDM 2023 | Link
S. Mehta. STS CF-Ladder Assembly & Vibrations. FTDM 2023 | Link
I. Eliazov. STS-FEE Cooling Plant. FTDM 2023 | Link

STS Cooling Concept

Silicon Sensors: Operating Temperatures

Factor #1: Reverse Annealing with time and temperature

- The STS sensors will operate at 500V at the EOL fluence to recover the charge collection efficiency, i.e., deposited charge
- The operating temperatures must be low enough not to invoke reverse annealing and keep the full depletion voltage sufficiently below 500V

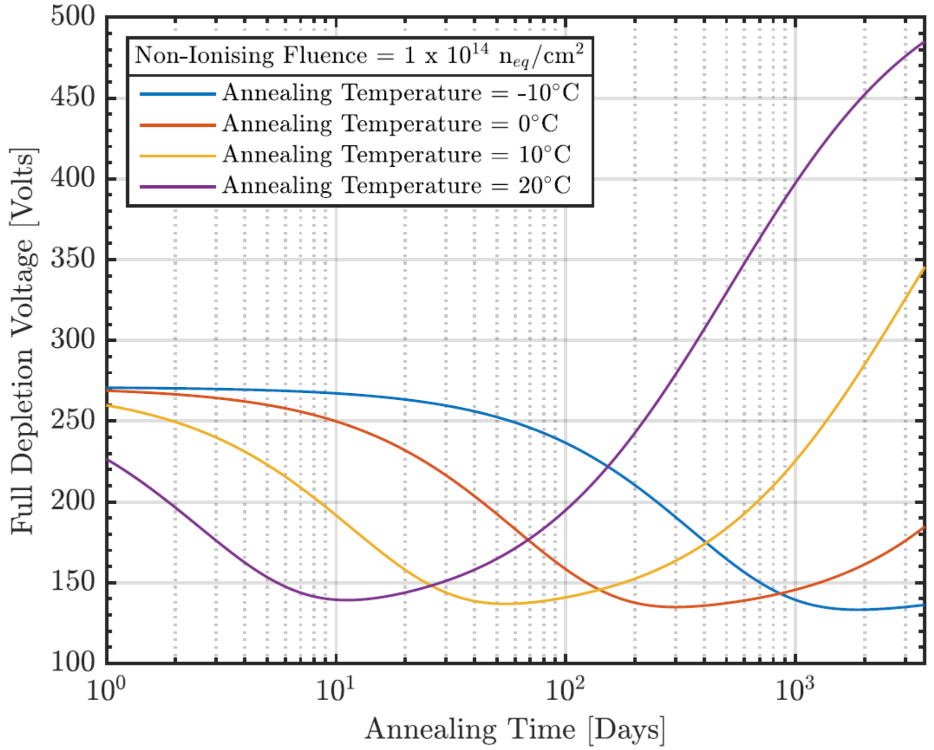

Based on Hamburg Model estimations for STS sensors as extracted in - P. Larionov, PhD Thesis, Universität Frankfurt (2016)

Factor #2: Signal-to-Noise Ratio (S/N) with time and fluence

- The STS track reconstruction requirements mandates that the S/N > 10
- The operating temperatures must be low enough to minimize the rise of shot noise at EOL fluence, thereby keeping S/N safely above 10

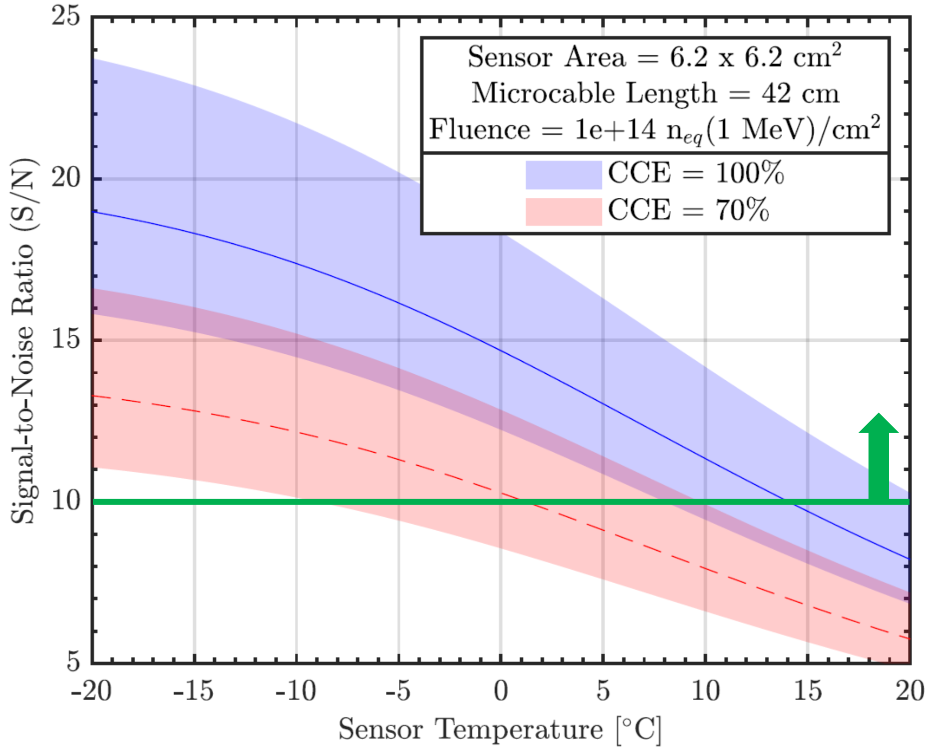

* For the innermost central module of the last STS station, i.e., with the longest sensor (6.2 x 6.2 cm^2) and microcables (42 cm) exposed to EOL fluence

** Error bands represent ±20% error in module's noise estimation from the analytical model

*** Cluster size = 1.52, therefore the noise is increased by $\sqrt{1.52}$

Based on the aforementioned factors, the STS sensors at their EOL fluence can be operated at 0...+10°C. Can the cooling cope up?

Silicon Sensors: Cooling Concept

- Only the innermost sensors ($\Delta x = \Delta y \leq \pm 10$ cm) on a given STS station will be exposed to EOL fluence
- The power dissipation of STS sensors is highly non-uniform and follows the fluence distribution (falls exponentially in radial direction)

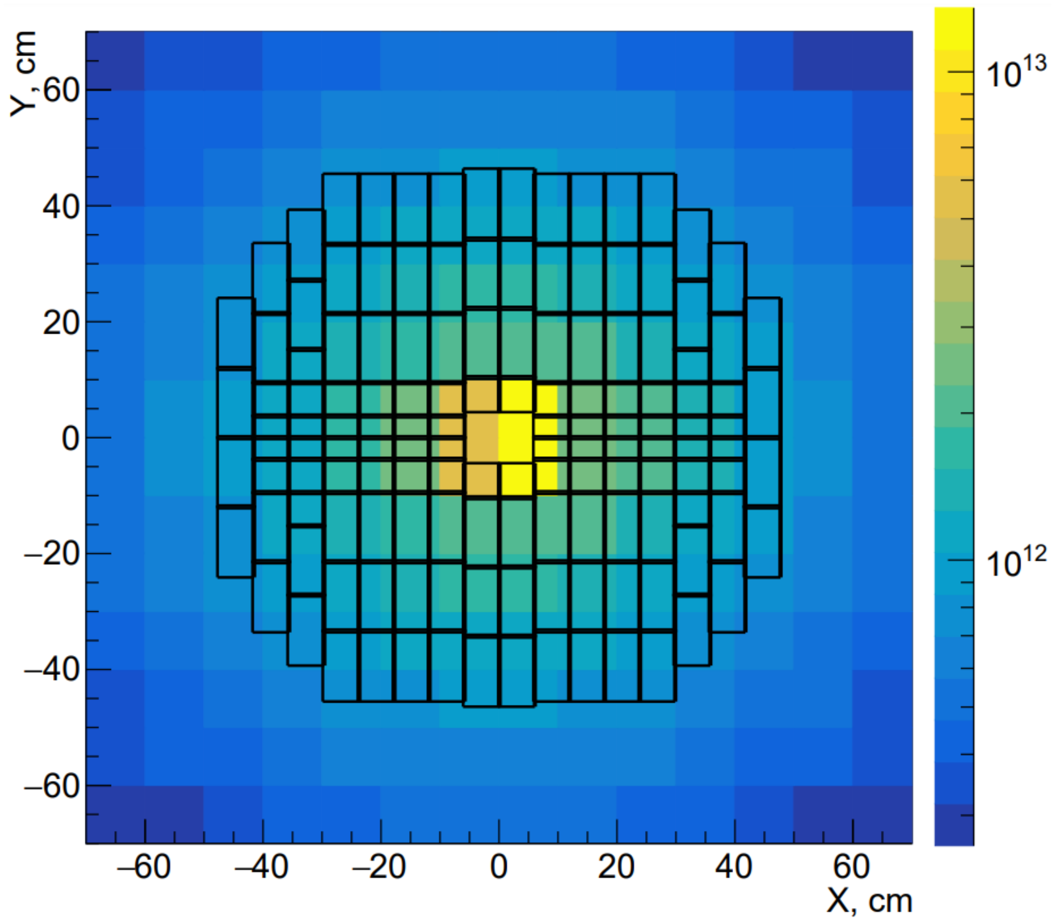

O. Bertini et al., CBM Progress Report 2020, pg. 216 (2021)

The innermost sensors of all stations are actively air cooled by perforated tubes based on concept of impinging jets and the peripheral sensors are air cooled by natural convection

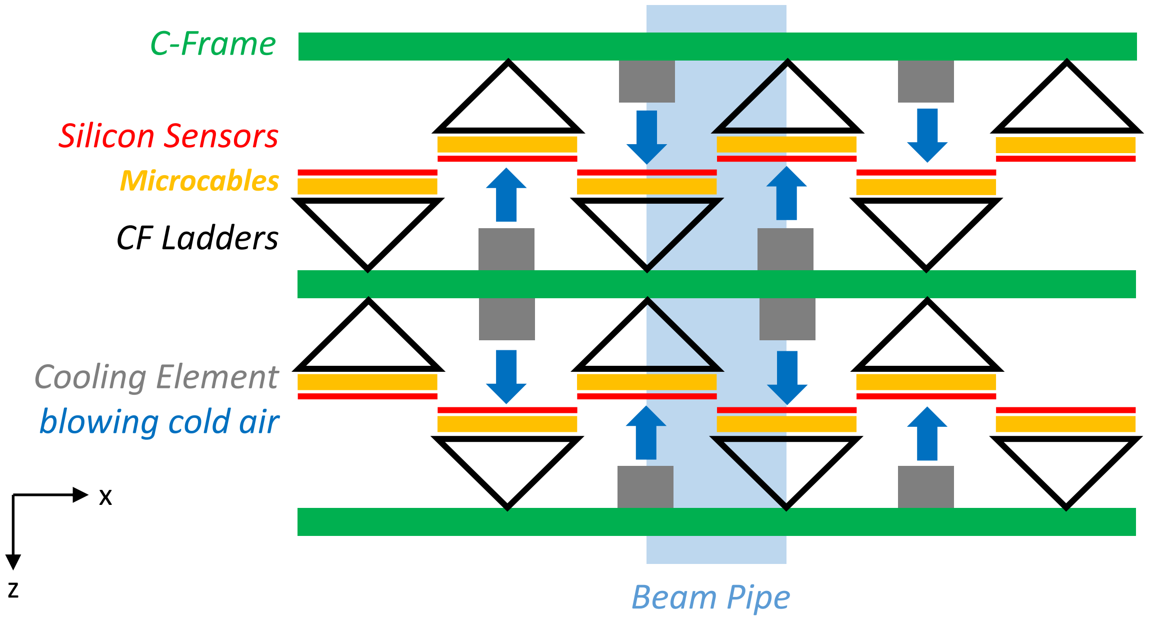

- Advantage: Low material budget, respective empirical formulations for both cases allow to predict the thermal behaviour (temp., runaway, …)

  Impinging Jets: H. Martin, Advances in Heat Transfer, 13 (1977)
  Natural Convection: S. W. Churchill and H. Chu, International Journal of Heat and Mass Transfer, 18.11 (1975)

- Perforated tube's geometry has been optimized within STS boundary conditions to reduce the tube diameter and ensure flow balancing amongst all perforations

Calculation details in backup

SILICON SENSORS: THERMAL RUNAWAY (CFD & CALCULATIONS)

Impinging air jets for centrally located ladders

- Ladder with the highest power dissipation in STS (6 mW/cm² at -10°C)
- Calculations and CFD simulations for different flow rates per perforated tube (20 … 40 L/min) and varying ambient air temperatures
- Reasonable agreement observed between calculations and CFD simulations for all considered cases

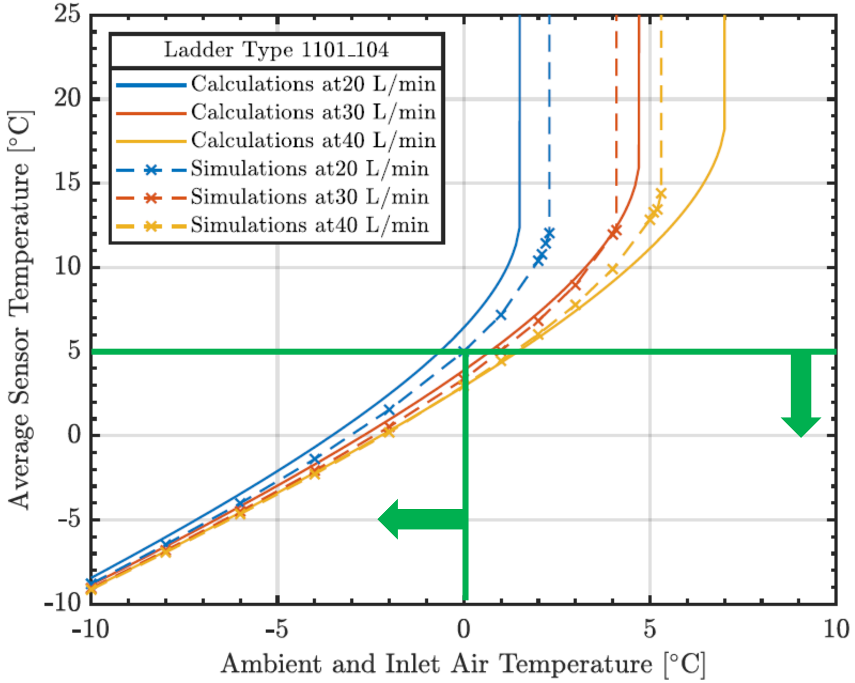

Natural air convection for peripherally located ladders

- Ladder with sensors with highest power dissipation to be cooled by natural air convection (0.37 mW/cm² at -10°C)
- Reasonable agreement observed between calculations and CFD simulations for all considered cases

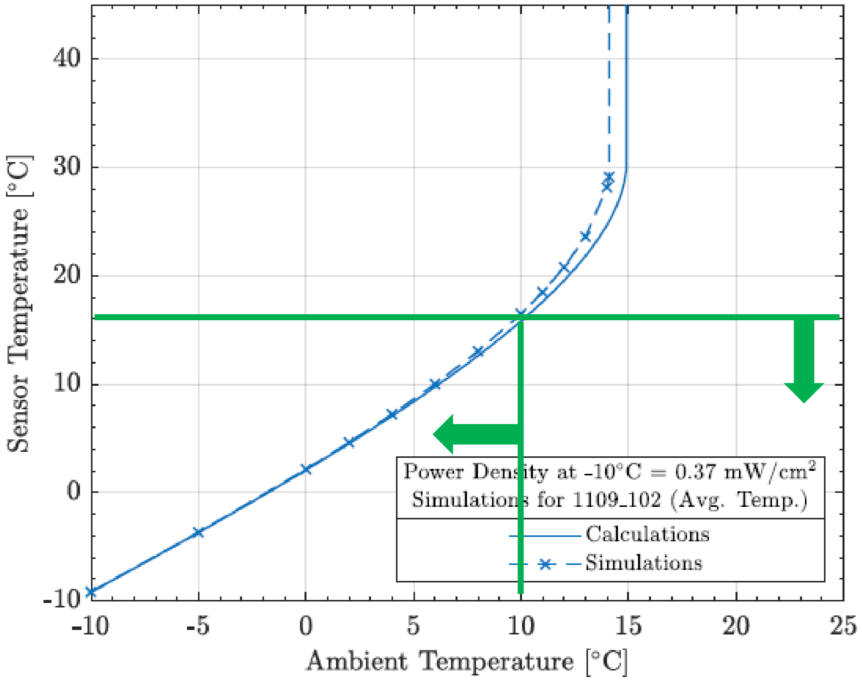

STS sensors can be safely operated at 0…+5°C at EOL fluence at ambient air temp. of 0°C with sufficient margin from thermal runaway.
Can the ambient air in the STS be kept at these temperatures by neutralizing other heat sources?

Front End Electronics: Cooling Concept [I]

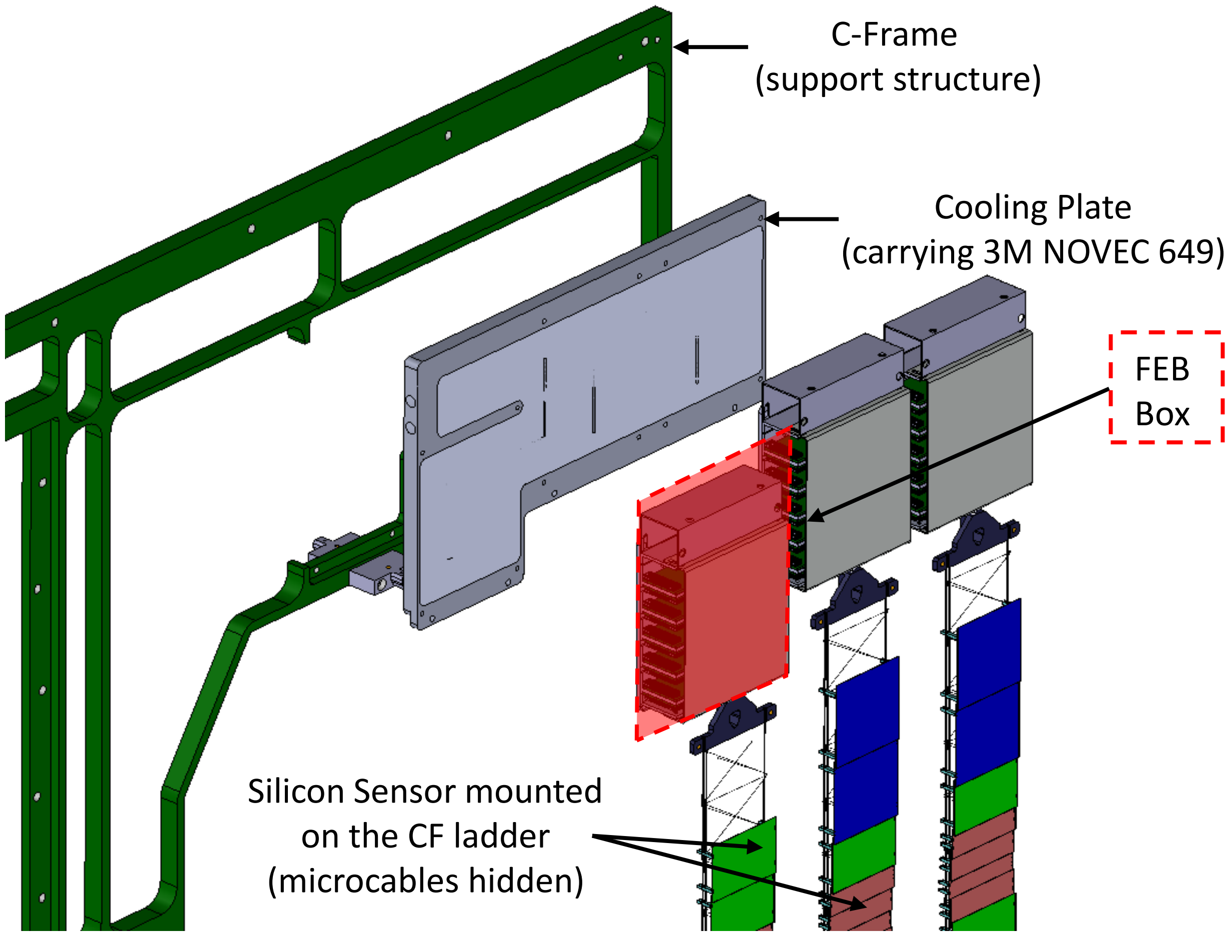

Since the FEB boxes carrying the FEEs are only 25…50 cm away from the innermost silicon sensors, the temperature gradient between the two must be minimal, i.e., FEEs should be at 0°C

Front-End Electronics Box (FEB-Box)

- FEB box host up to 5 fins/10 front-end electronics boards (FEBs), with total power dissipation of approx. 100 W
- Provide a thermally conducting pathway to the cooling plate
- Modular design with several thermal interface materials (TIMs)

S. Mehta. STS Module Assembly and TIMs. FTDM 2022 | Link

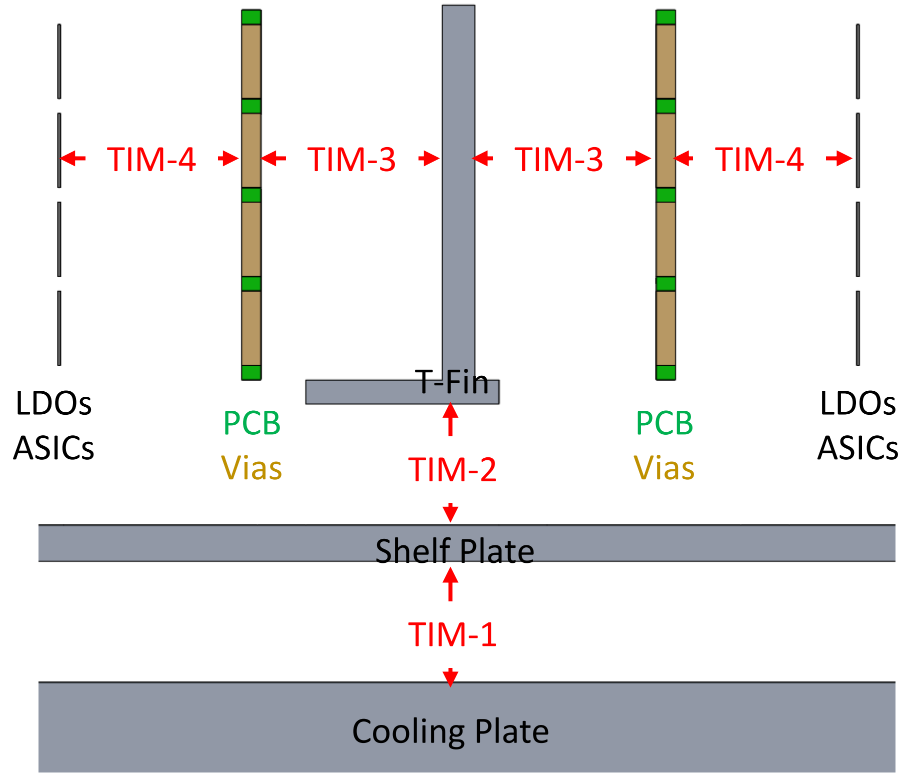

FRONT END ELECTRONICS: COOLING CONCEPT [II]

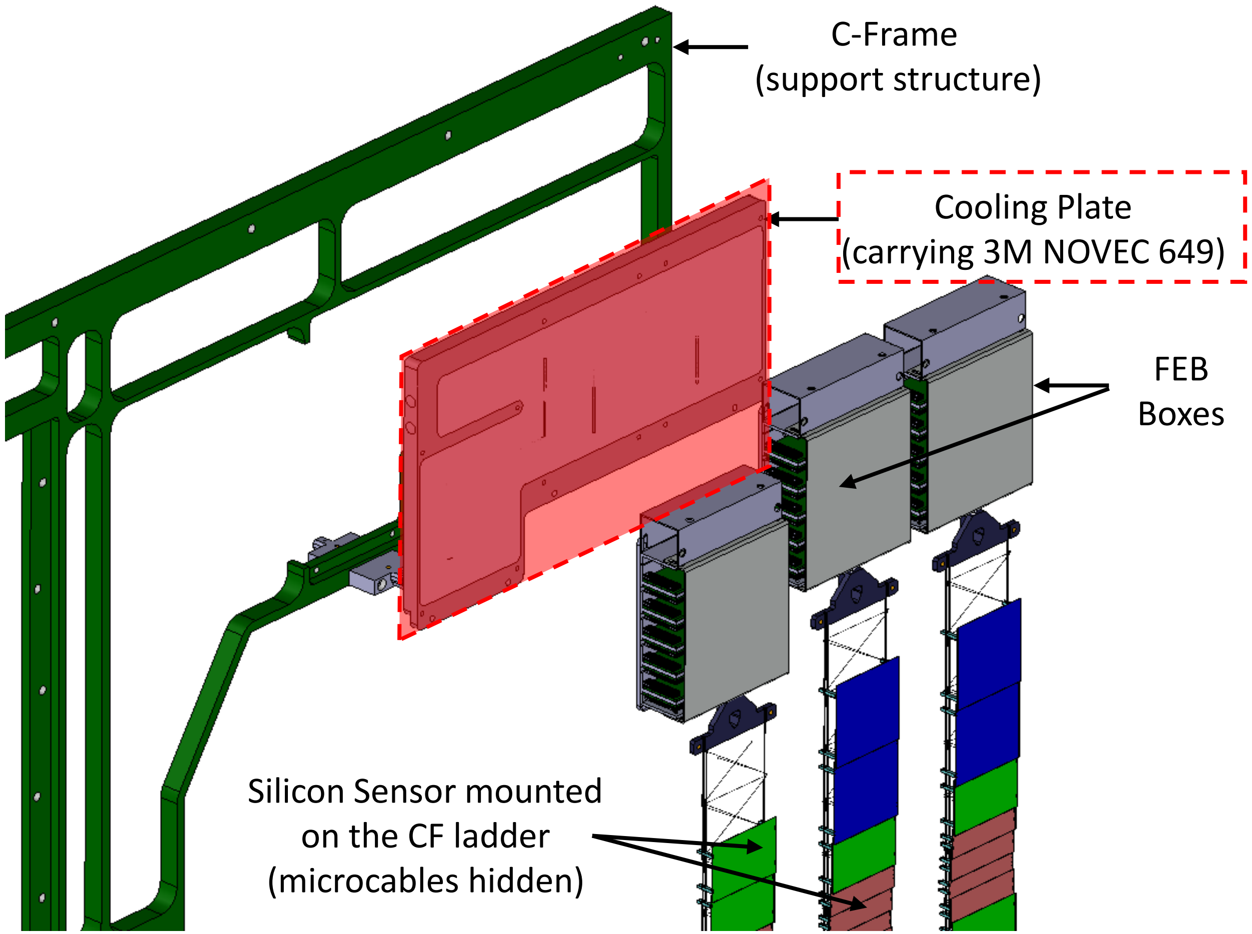

Since the FEB boxes carrying the FEEs are only 25…50 cm away from the inmost silicon sensors, the temperature gradient between the two must be minimal, i.e., FEEs should be at 0°C

Cooling Plate

- Cooling plates are foreseen to remove power dissipation of up to 1 kW
- Coolant to be used here – 3M NOVEC 649
- Plates manufactured by “Friction Stir Technology”
  - Flexibility to add threaded connections for inlet-outlet
  - Flexibility to mill fluid channels to enhance local heat transfer co-efficient and cooling performance
- Maximum bulging on the cooling plate under 5 bar(g) is < 100 µm

Measurement details in backup

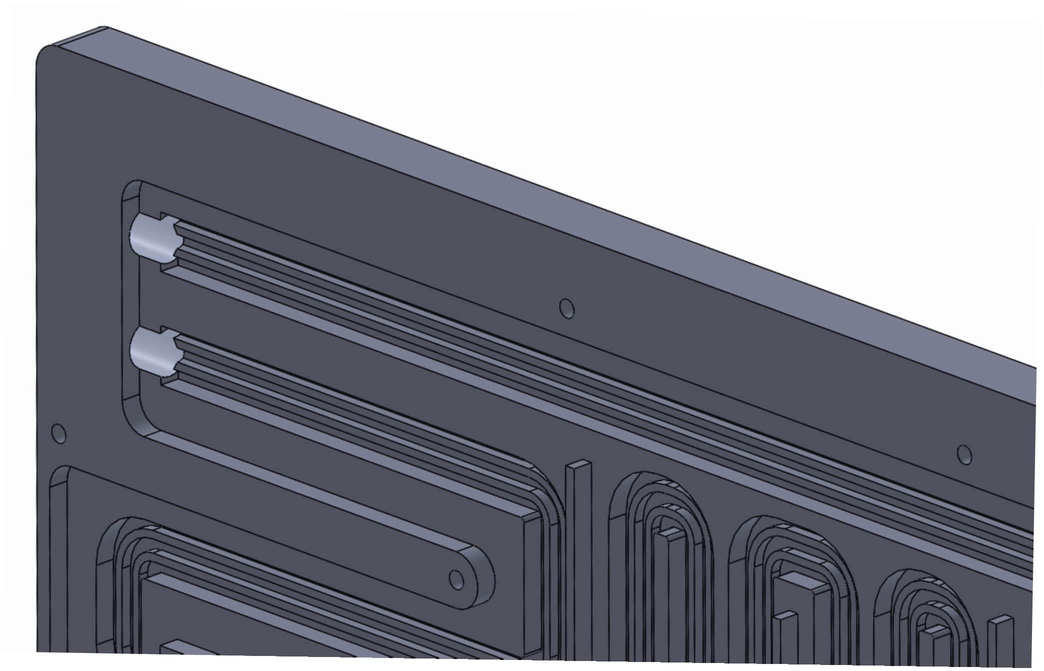

FRONT END ELECTRONICS: CFD & THERMAL SIMULATIONS

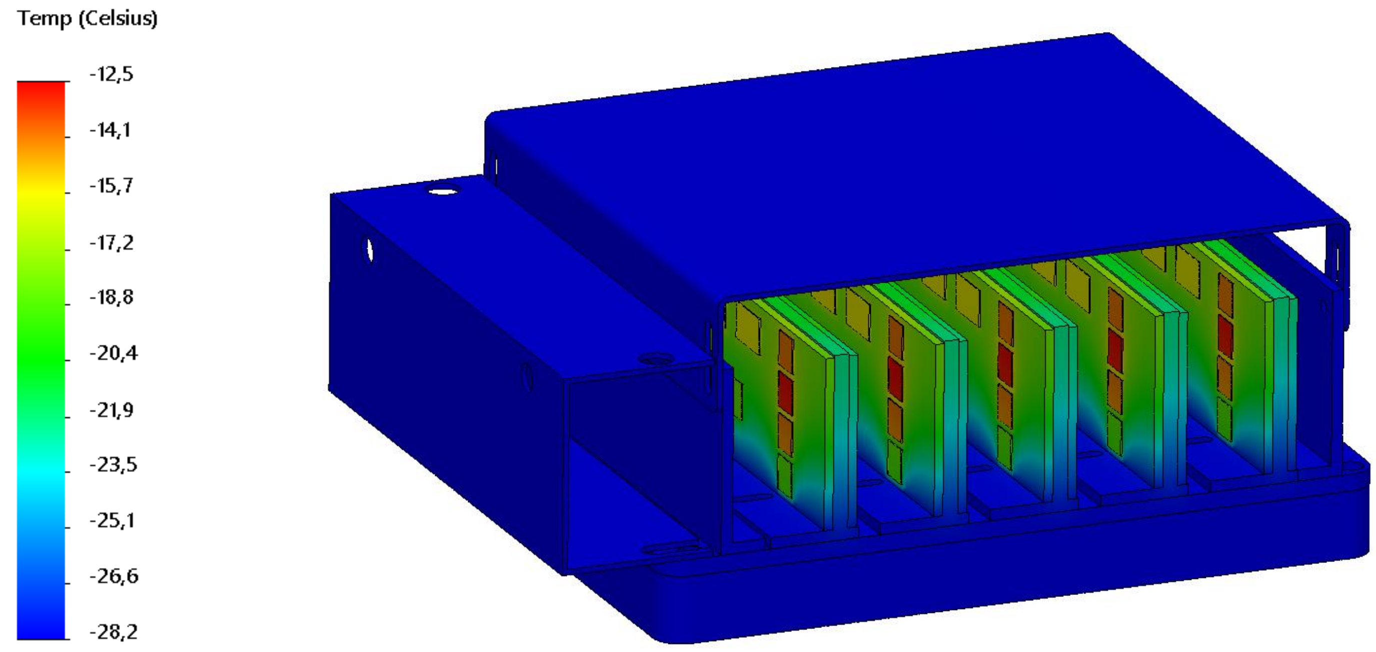

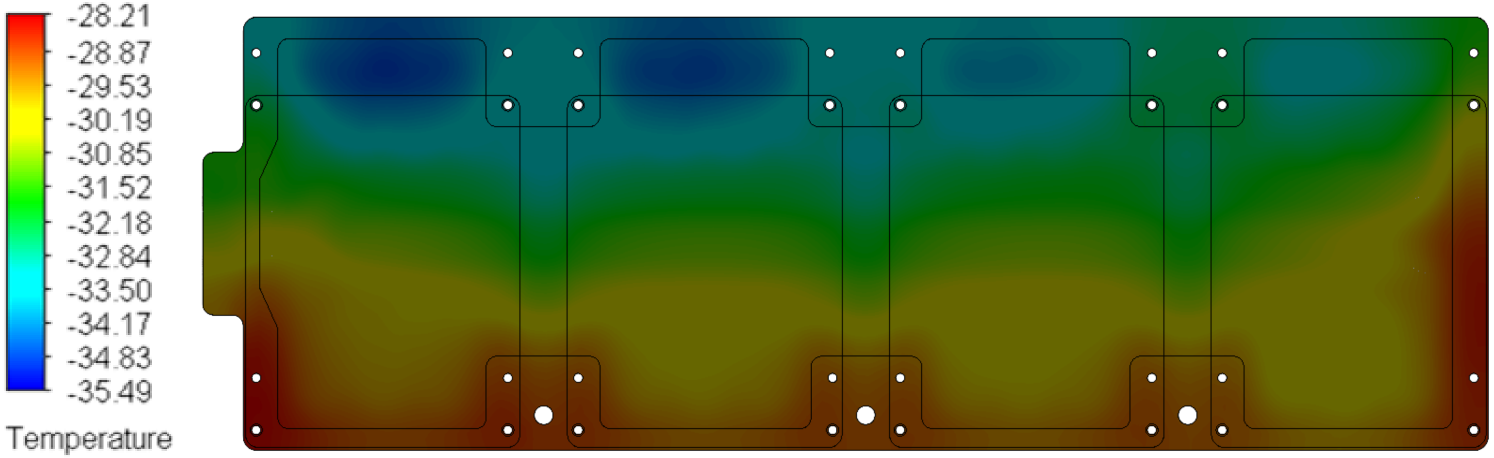

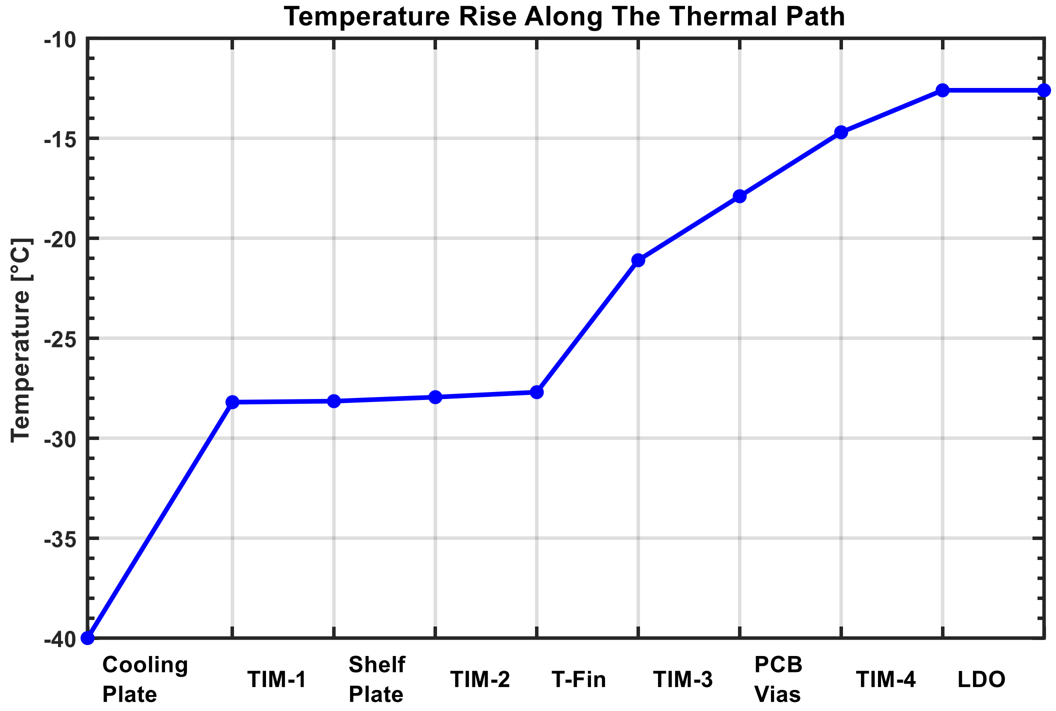

A combination of CFD simulations for the cooling plate and thermal simulations for the FEB box show that the coolant temperature of -40°C leads to the max. FEB temp. of < -10°C

What is the interplay between the coolant/FEB temp. and the silicon sensors?

Experimental Verification
- Thermal Demonstrator -

THERMAL DEMONSTRATOR: CONCEPT

Thermal demonstrator aims to experimentally verify the sensor and FEE cooling concept under (quasi-)realistic boundary conditions

- Three STS-like half-stations with one "active" layer (power dissipation of approx. 1 kW) sandwiched between two "passive" layers
- Sensor cooling done with perforated CF-tubes
- FEE cooling done with 3M NOVEC 649
- Dummy silicon sensor heaters and FEE heaters
- STS-like peripheral services, such as electronics and coolant feedthroughs, coolant manifold, valves and transfer lines
- CF-AIREX based thermal enclosure, with actively cooled panels

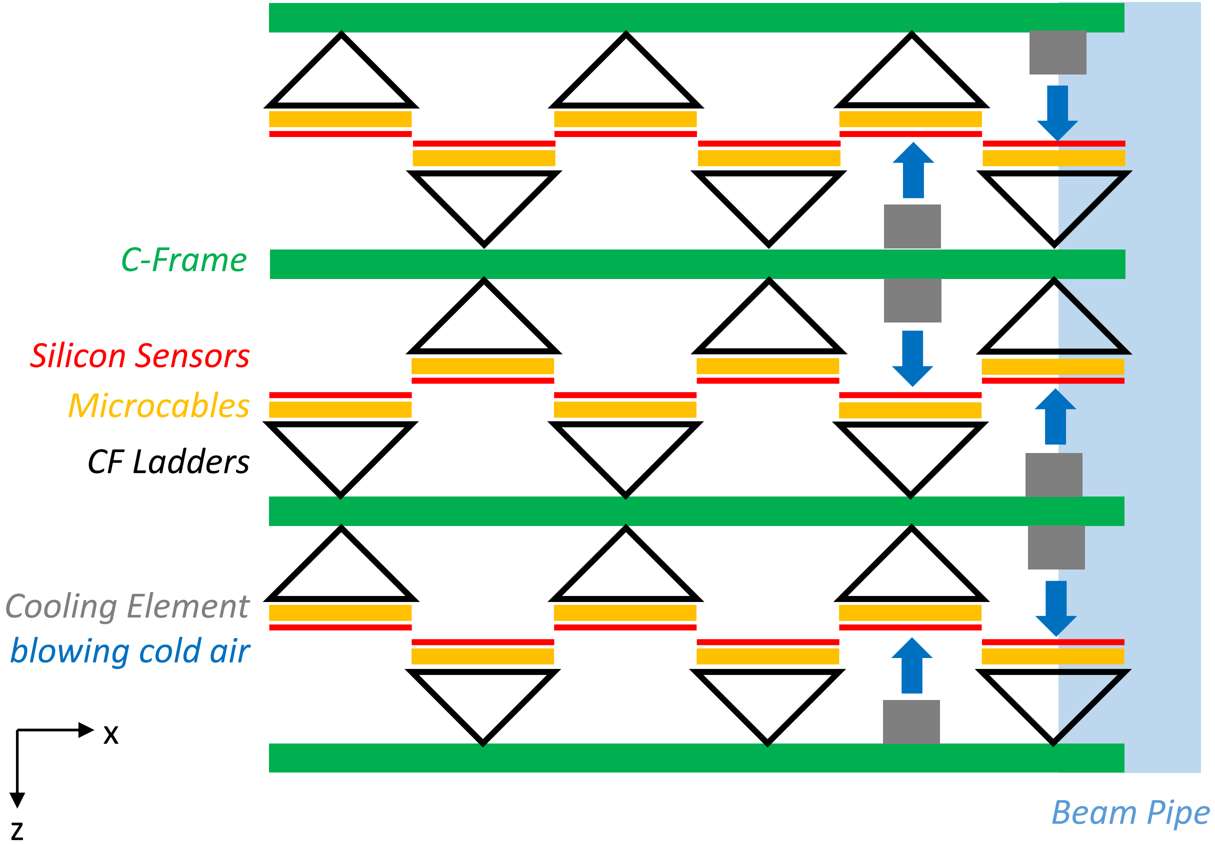

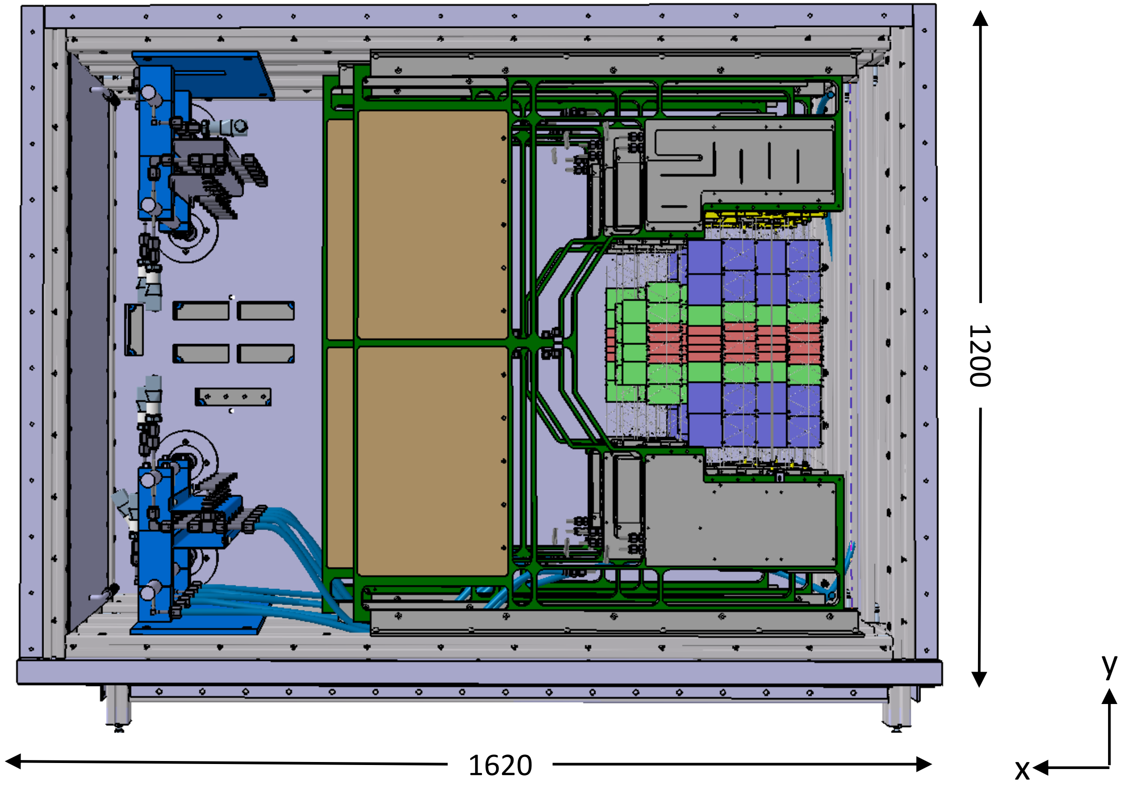

Thermal Demonstrator: Components [I]

Realistic Heat Sources

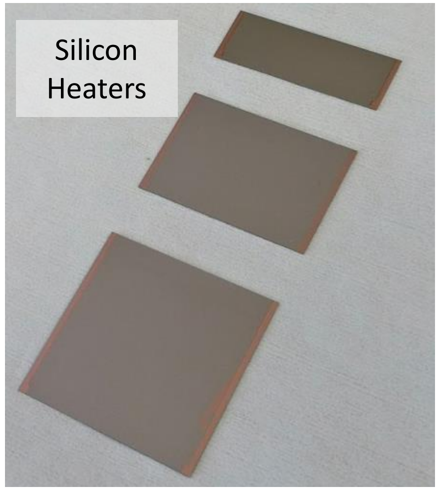

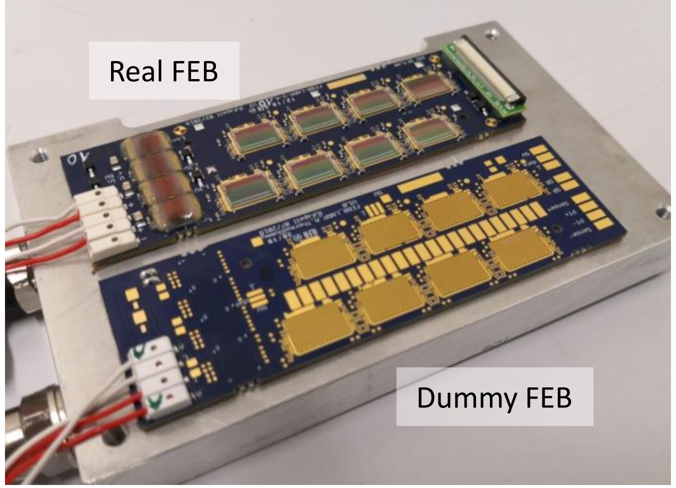

Humidity Monitoring System

C-Frame assembled with heat sources mounted on ladders, along with cooling elements and power distribution

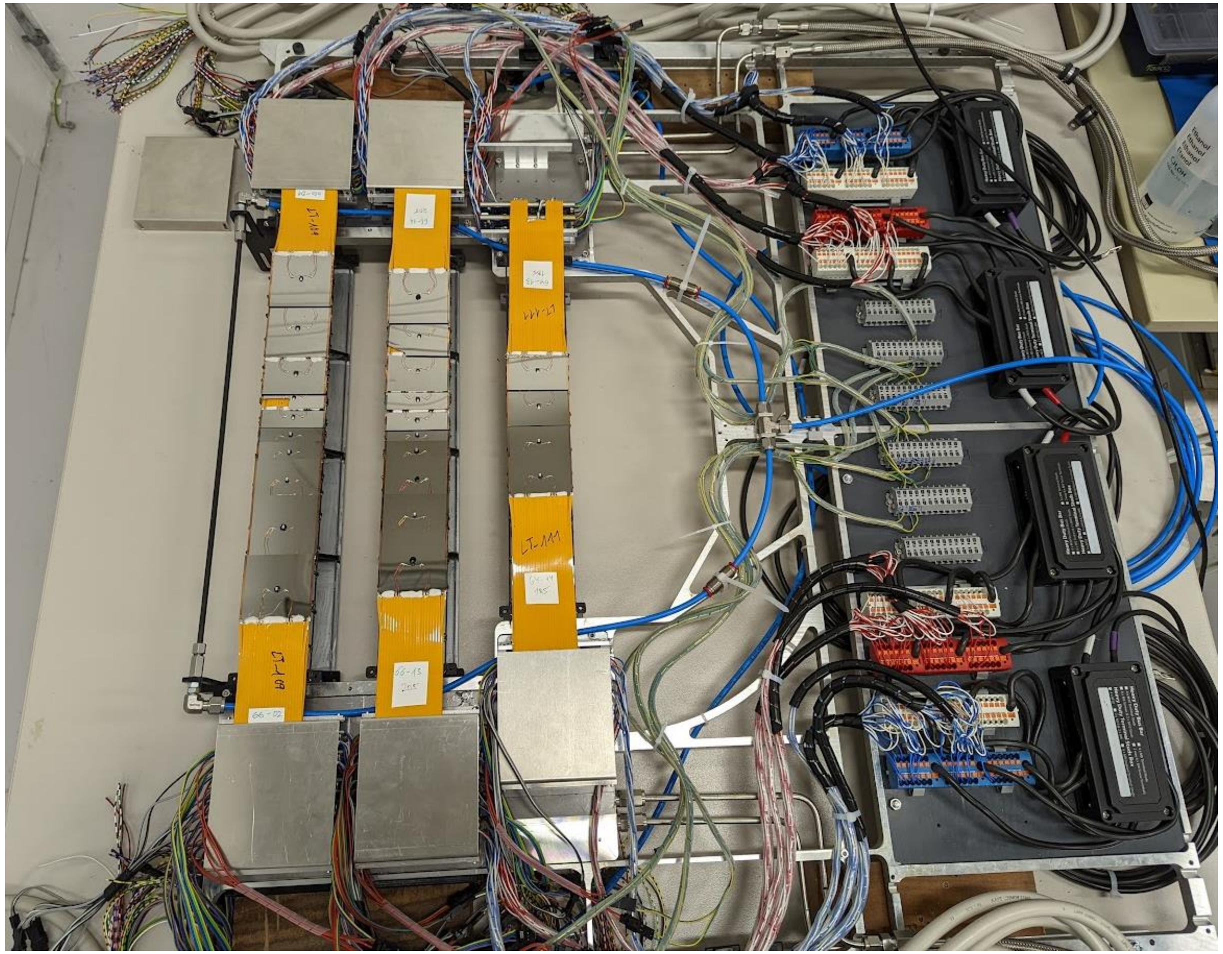

THERMAL DEMONSTRATOR: COMPONENTS [II]

NOVEC Manifold and Feedthroughs

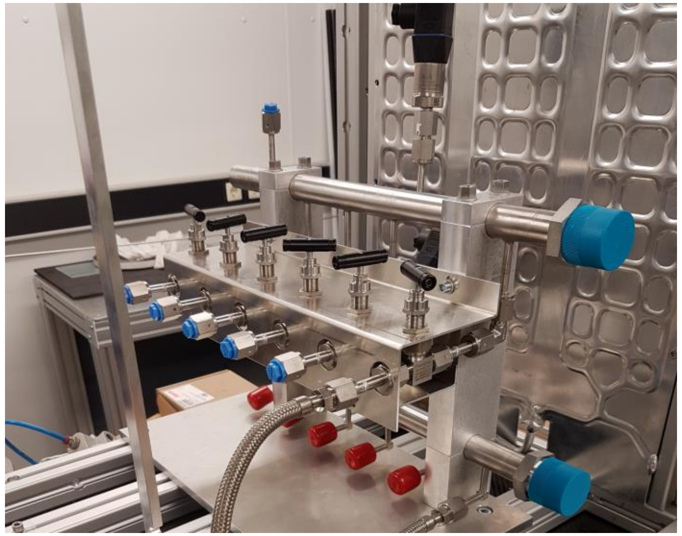

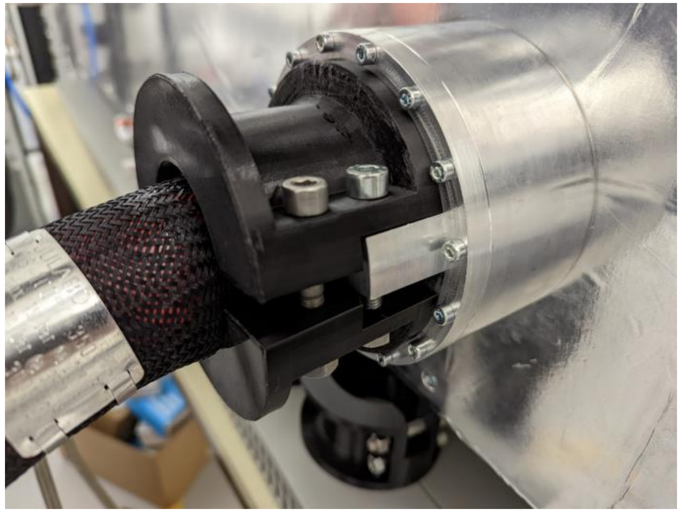

Thermal Enclosure made from CF-AIREX sandwich panels, cladded with aluminised-Kapton sheets and cold plates on the side panels

THERMAL DEMONSTRATOR: COMPONENTS [III]

NOVEC Chillers

Option #1
Julabo Presto W50
(-20 … +20°C)

Option #2
Custom-made NOVEC Chiller (CO_2 in primary cycle)
(-40 … -20°C)

I. Eliazov. STS-FEE Cooling Plant. FTDM 2023 | Link

Air Handling System

Dry Air Dewpoint = down to approx. -70°C
Cold Air Temperature= -15 … +30°C

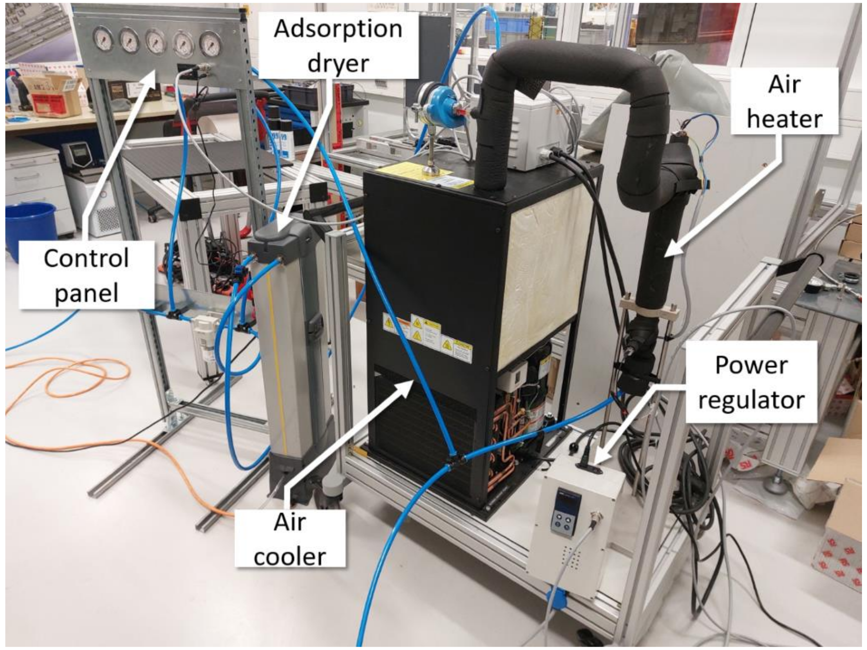

THERMAL DEMONSTRATOR: CONCEPT & COMPONENTS [V]

STS Thermal Demonstrator – Assembled and Running… ☺

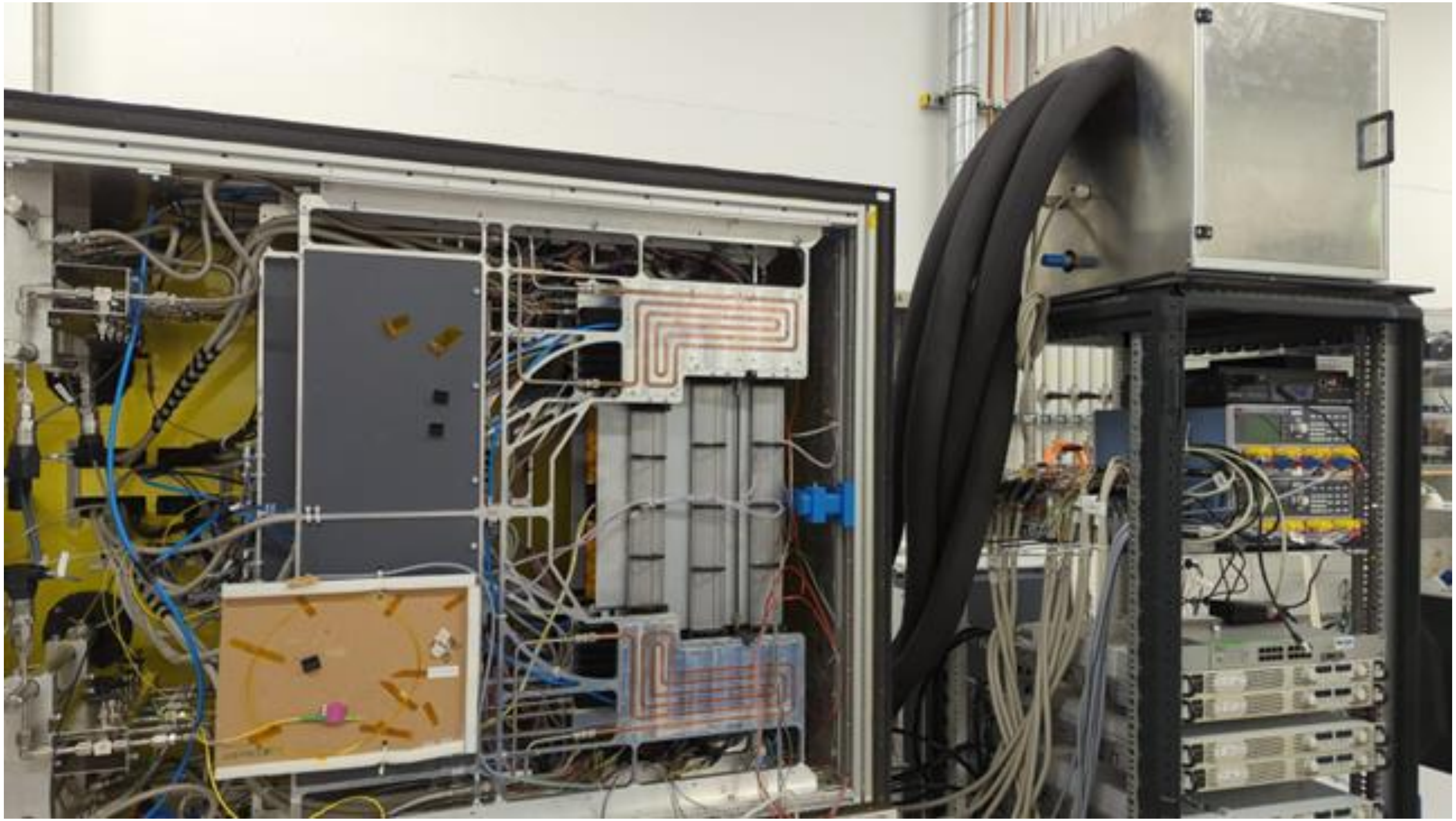

First Results: Thermal Runaway Behaviour At EOL Fluence

- FEE Power Dissipation = Approx. 1 kW
- NOVEC Temperature = -20°C (Julabo Presto W50)

- Ambient Dew Point = below -70°C
- Ambient Overpressure = 12…13 mbar
- Cold plates on side panels OFF

- Inlet Air Temperature = 24…25°C

- Sensor power dissipation across the half-station varied proportional to the expected EOL radiation damage distribution

When using perforated-tube based active air cooling, the innermost STS sensors can be safely operated at 9°C at EOL fluence with sufficient margin from thermal runaway while using NOVEC at -20°C

S. Mehta. STS CF-Ladder Assembly & Vibrations. FTDM 2023 | Link

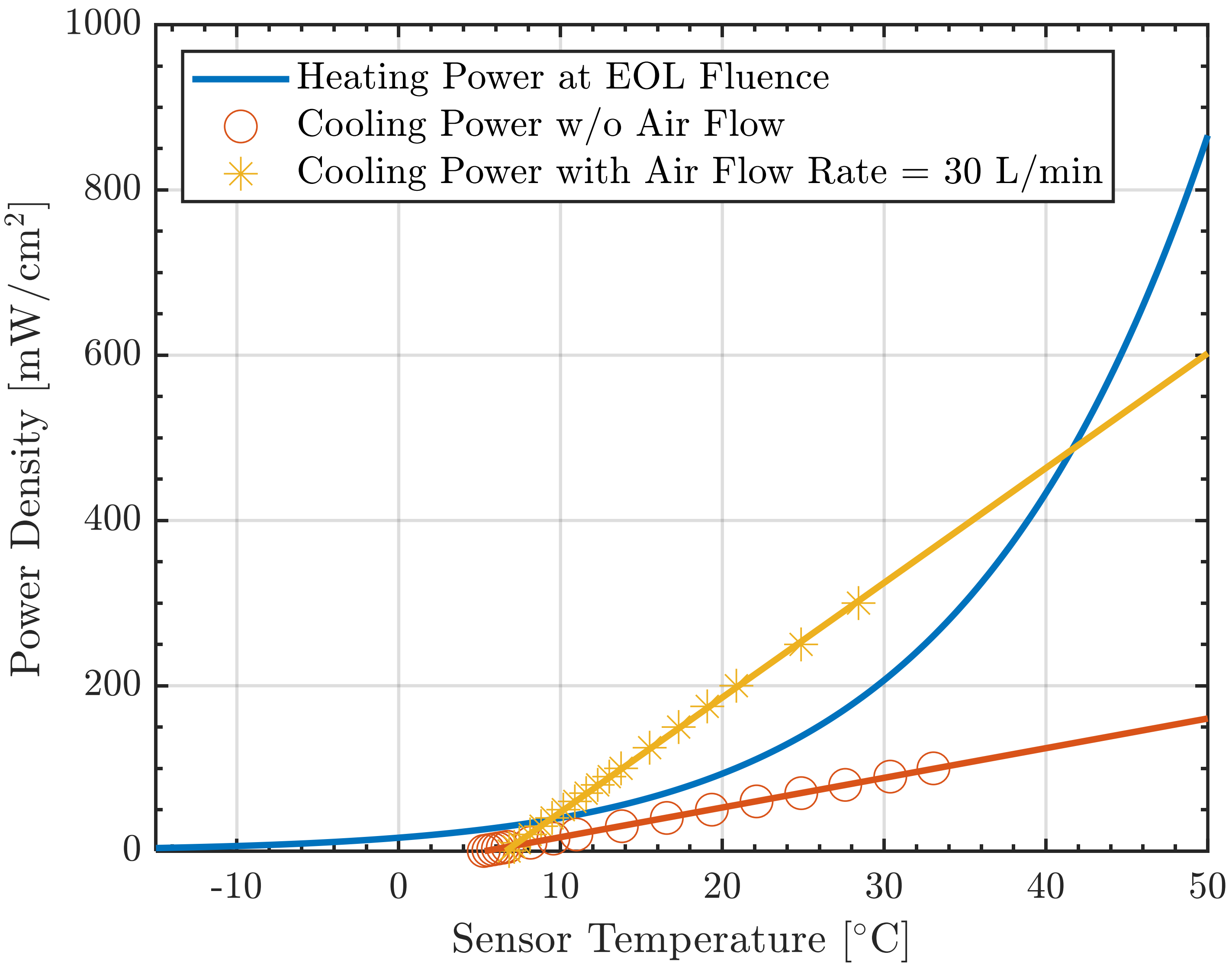

Summary And Outlook

- STS Cooling Concept
  - Silicon sensors are to be operated at 0…+10°C to avoid reverse annealing and maintain high signal-to-noise ratio at the end-of-lifetime fluence
  - Theoretical calculations and CFD simulations show that the impinging jets-based CF perforated tubes can cool away the silicon sensors with sufficient margin from thermal runaway
  - Thermal and CFD simulations show that the 3M NOVEC 649-based FEE cooling can reliably cool down the front-end electronics (up to 40 kW power dissipation)

- Experimental Verification
  - Thermal Demonstrator with three STS-like half-stations has been assembled to verify the sensor and FEE cooling concept under (quasi) realistic boundary conditions
  - First results show that upon neutralising the FEE power dissipation with 3M NOVEC 649 at -20°C, the STS sensors can be safely operated at approx. 9°C with sufficient margin from thermal runaway by using impinging jets

- Outlook and Future Plans
  - Role of cold plates on the side panels (i.e., better thermal insulation) to be studied
  - Further operational phase space of the thermal demonstrator to tested by performing NOVEC temperature scan from -40 … - 20°C using STS Pilot Cooling Plant and various air flow rates (0…40 L/min)

Thank You

CBM

Acknowledgements: Entire CBM-STS Working Group and FTDM Community (too many people to list …) _/_

compact KÄLTETECHNIK | KKR GmbH Klima-Kälte-Reinraumtechnik | Cool Tec Electronic GmbH | ICM-Composites | sumida | Roxtec | Swagelok | DEMACO

SILTRONIX silicon technologies | Julabo The Temperature Control Company | ILFA | RUBANOX EST.1913 | DSN Thermal Solution | CarbonVision | item | CGS Creative Global Services Inc. Specialize In Polyimide Tape & Film

CBM-FAIR

Facility For Anti-Proton And Ion Research (FAIR)

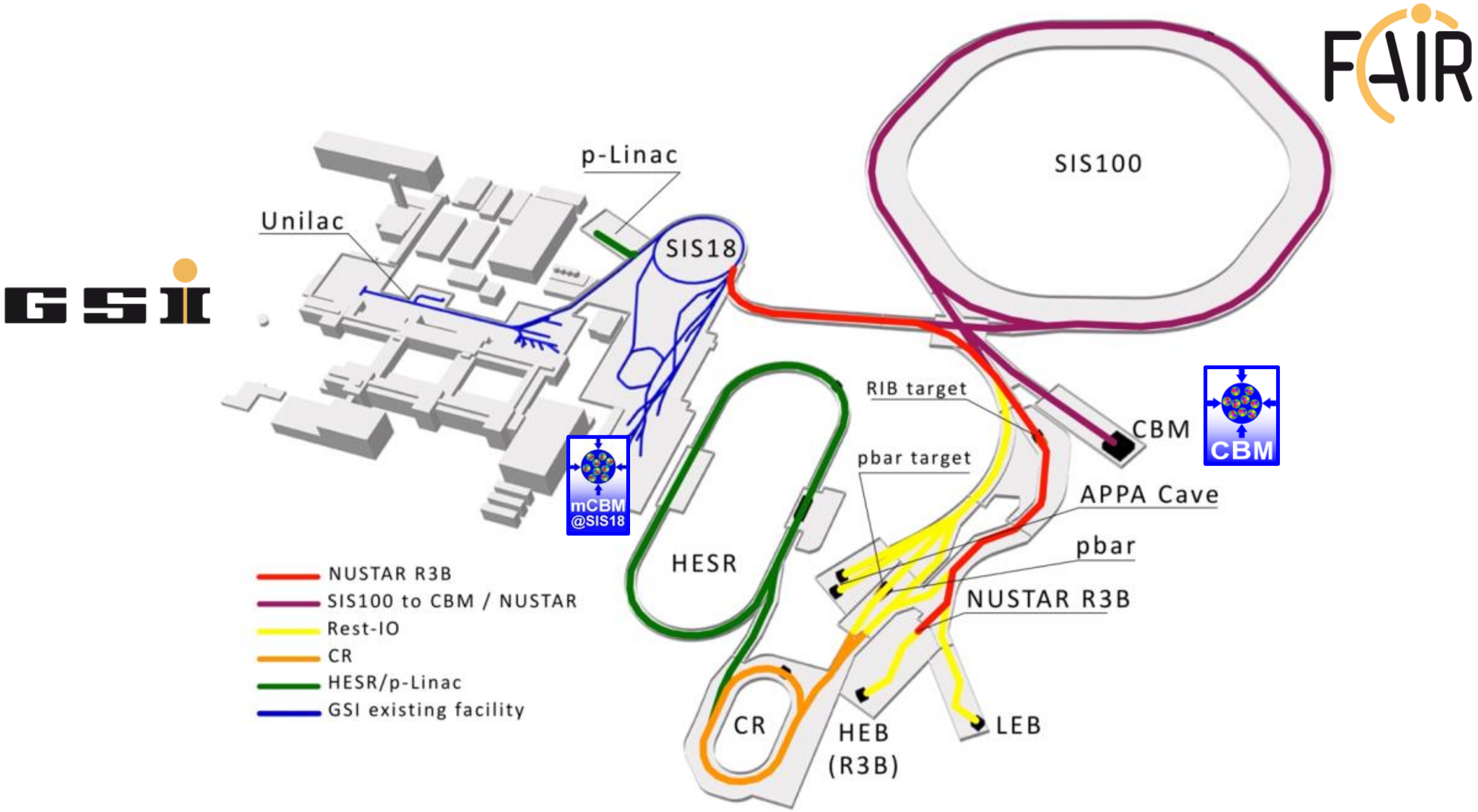

SIS-100 Capabilities			
Beam	Z	A	E_{max} [AGeV]
p	1	1	29
d	1	2	14
Ca	20	40	14
…			
Au	79	197	11
U	92	238	10.7

C. Höhne et al. (2011) CBM Experiment. In: B. Friman (eds) The CBM Physics Book. Lecture Notes in Physics, vol 814. Springer

M. Durante et al., Phys. Scr. 2019, 94, 033001

- Intensity gain: x 100 – 1000 (~10^9/s for Au)
- Energy gain: 10 x energy (compared to SIS-18@GSI)
- Antimatter: antiproton beams
- Precision: System of storage and cooler rings

- Current estimate: SIS100 commissioning with beams starts in 2028-29
- Recommendation from Heuer-Tribble Committee: downscale FAIR project (SIS100 & SFRS/R3B & CBM); Decision by FAIR council expected in Feb. 2023

GSI Press Release – Link
Report PDF – Link

Vote Of Confidence For CBM-FAIR

Report

from the Committee for

First-Science and Staging Review of the FAIR Project

Submitted to FAIR Council, October 2022

GSI Press Release – Link
Report PDF – Link

The committee came unanimously to the following recommendations in order to advance FAIR to science beyond Phase-0:

- First priority should be the completion of the S-FRS into the HEB cave for NUSTAR to carry out the Early Science program.
- Completion of SIS100 needs to have the next highest priority.
- If resources are tightly constrained, completing SIS100 with beams into the S-FRS and HEB cave, plus setting up and commissioning the CBM experiment offers an intermediate solution for developing world-class science at FAIR.
- Completing the infrastructure and instrumenting the APPA cave should have priority over instrumenting the additional area in LEB for NUSTAR.
- Tendering for civil construction of the West lot should be postponed, but a plan is needed for the time frame to implement PANDA.
- The orderly set of steps towards the IO, presented in this document, represents the most cost-effective plan for moving FAIR forward. In order to accomplish this, a yearly budget

- The Heuer-Tribble Committee suggests a stepwise approach for the realization of FAIR
- Completion of SIS-100 was noted to be “existential” to FAIR
- Further endorsement obtained that bringing CBM to life will extend FAIR’s first science programme at a “minimal cost”

CBM Physics Goals

[STAR], Studying the Phase Diagram of QCD Matter at RHIC, STAR Note 598 (2014)

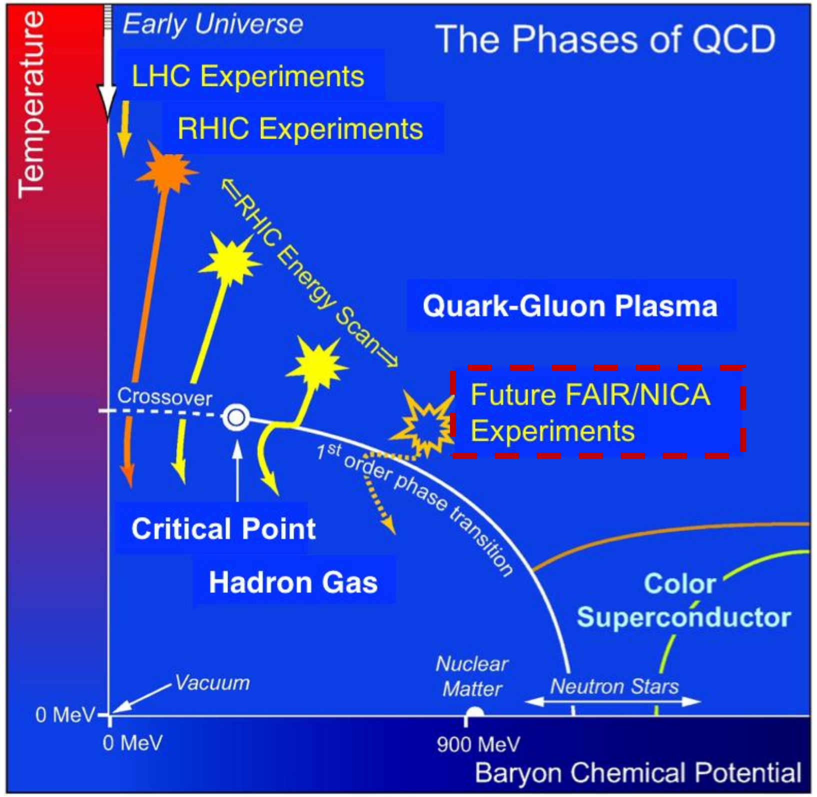

<u>Unanswered fundamental questions for QCD at high densities</u>

- Equation of State (EoS) of symmetric nuclear (and asymmetric neutron) matter at neutron star core densities
- Phase structure of QCD matter (1st-order phase trans.? critical point?)
- Chiral symmetry restoration at large μ_B
- Bound states with strangeness
- Charm in cold and dense matter

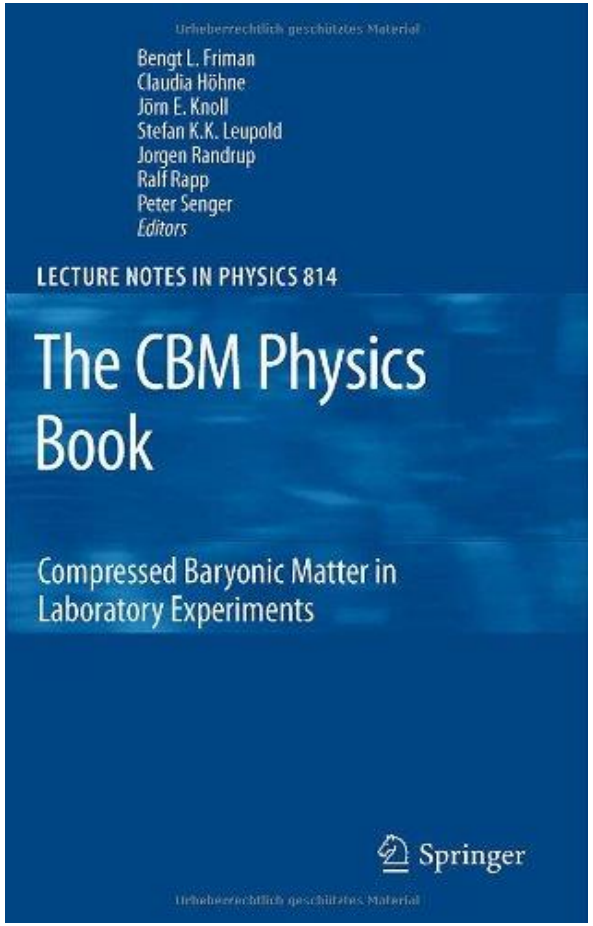

Lect. Notes Phys. 814 (2011) pp.1-980
DOI: 10.1007/978-3-642-13293-3

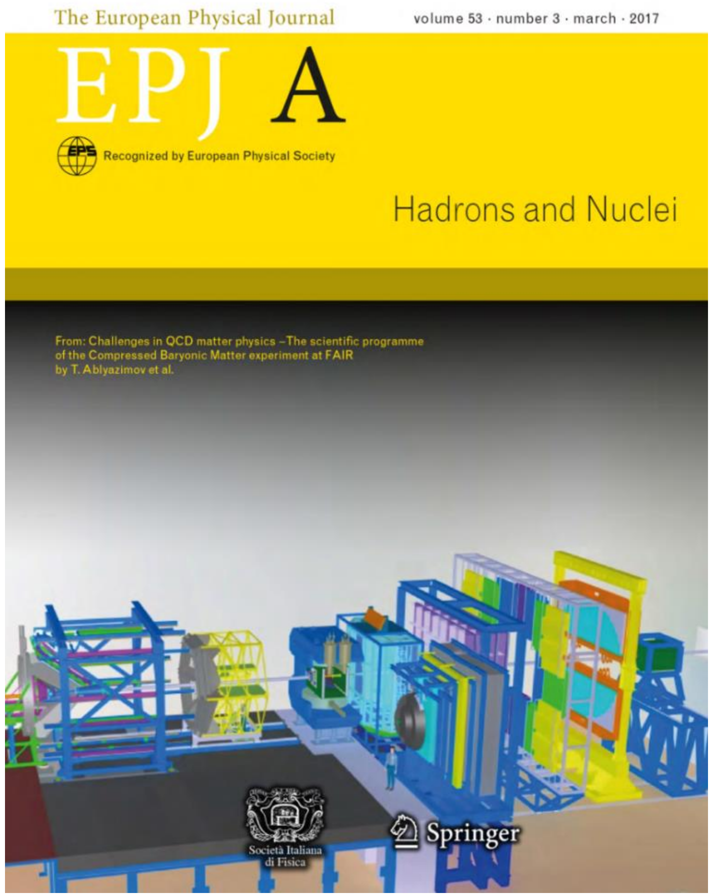

Eur.Phys.J.A 53 (2017) 3, 60
DOI: 10.1140/epja/i2017-12248-y

RECENT (& BRIEF) ACHIEVEMENTS IN DETECTOR PROJECTS

Beam Monitoring (BMON) Detector

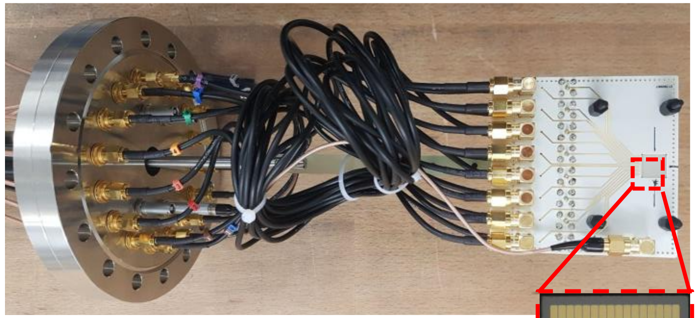

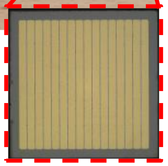

pcCVD diamond sensor (16-ch)
for high-intensity tests

Superconducting Dipole Magnet

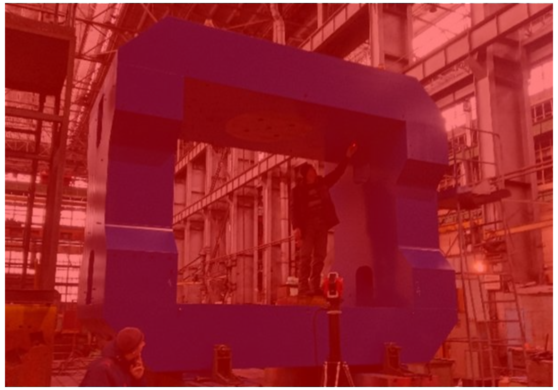

Magnet Yoke housed in BINP (Russia).
Tendering for replacement started.

Micro-Vertex Detector (MVD)

MVD's TDR accepted.
Improved MIMOSIS-2 being submitted.

Silicon Tracking System (STS)

Pre-series STS module production for E16 (J-PARC) exp.

Muon Chambers (MUCH)

RPCs at tested at nominal
rates at GIF++ (Nov.21)

Ring Imaging Cherenkov (RICH) Detector

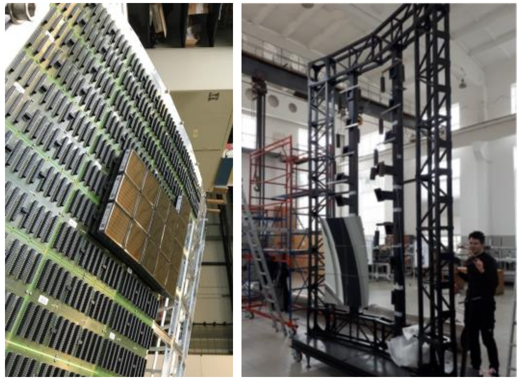

Photocamera and Mechanical
Prototypes (Mirror Wall)

Transition Radiation Detector (TRD)

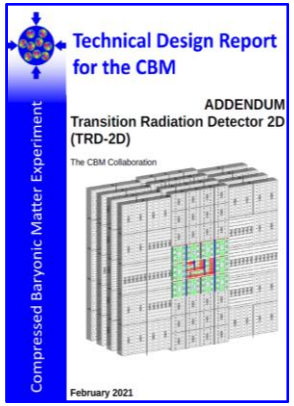

TRD-2D-addendum submitted.
TRD-1D pre-production by Q1-2023.

Time-of-Flight (ToF) Wall

Full-size counters (all types) built and tested
for high-rate and longer-term tests

Projectile Spectator Detector (PSD)

Efforts to replace PSD with
HADES-like FWALL. Still open issue.

STS Sensor Cooling

SENSOR COOLING CONCEPT (JETS AND CONVECTION)

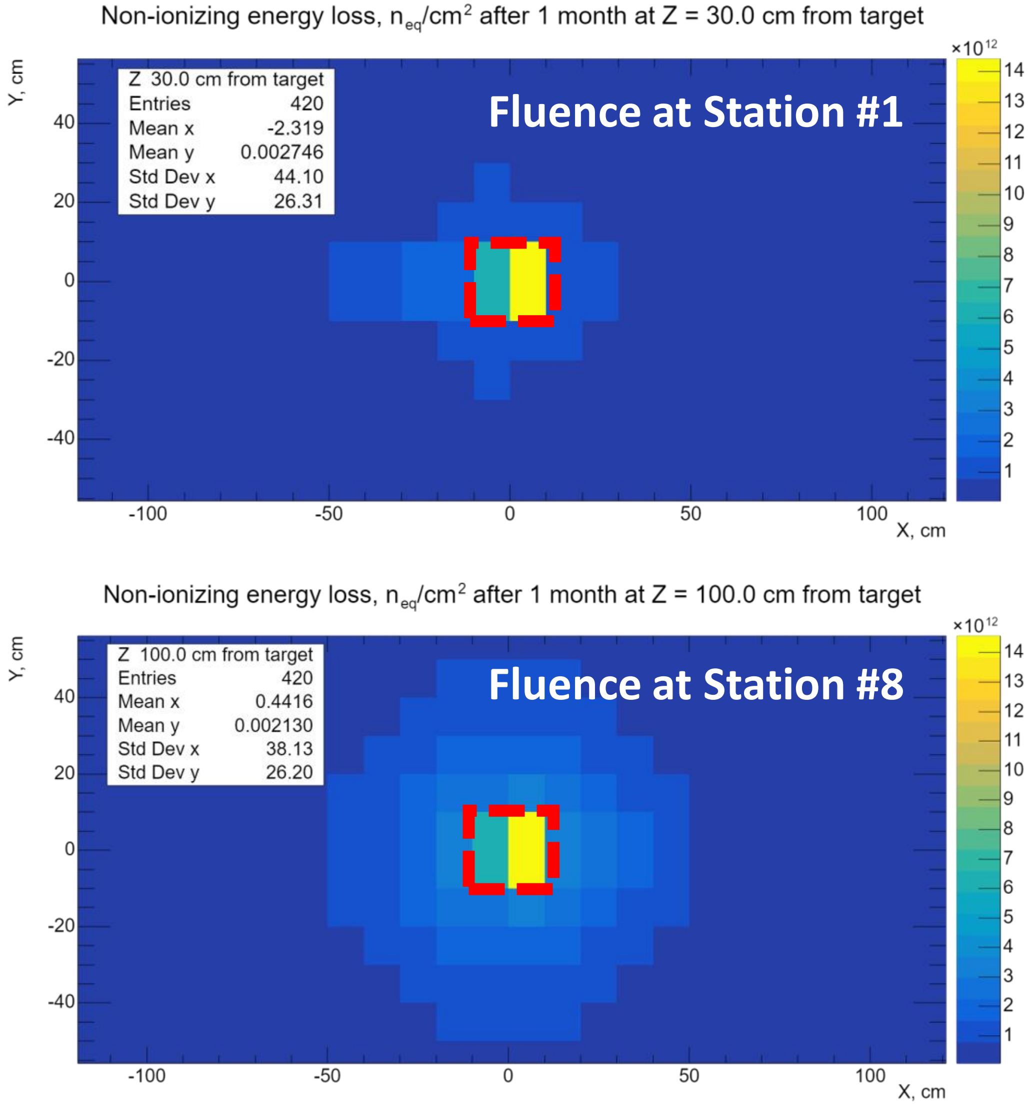

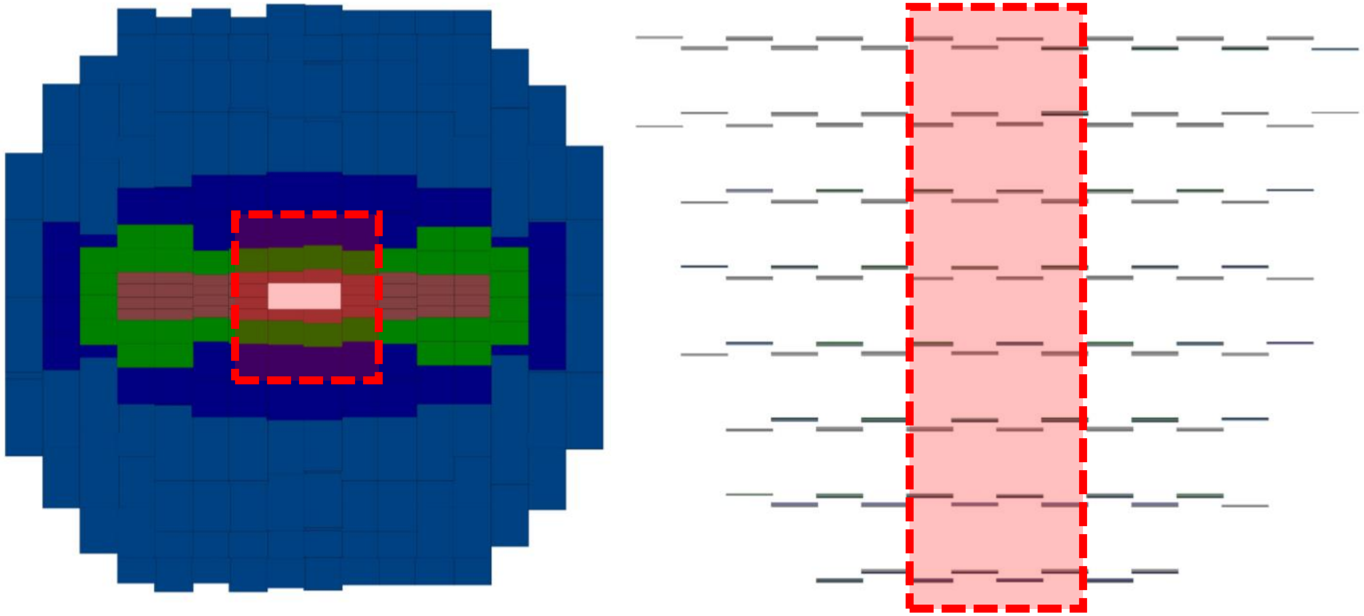

STS Front View

STS Top View

- **Only the innermost sensors of all stations (x,y ≤ ± 10 cm → 4 ladders) requires active cooling because of the higher fluence or higher power dissipation (> 1mW/cm² at -10°C)**
- **The peripheral sensors of all stations are aimed to be cooled by natural convection**

Online Tool: ***https://fair-center.eu/fileadmin/fair/experiments/CBM/tmp/CBM_FLUKA.htm***

SENSOR COOLING CONCEPT (JETS AND CONVECTION)

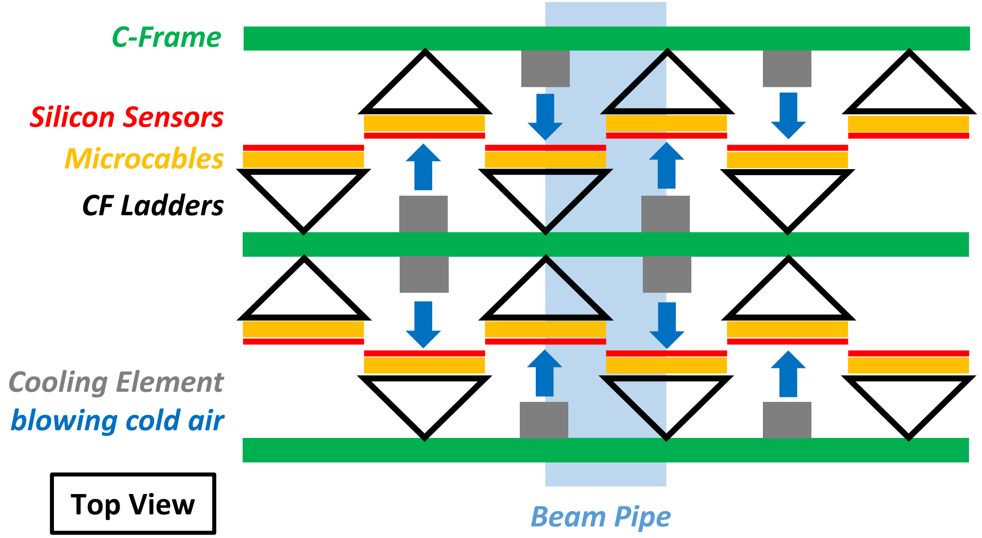

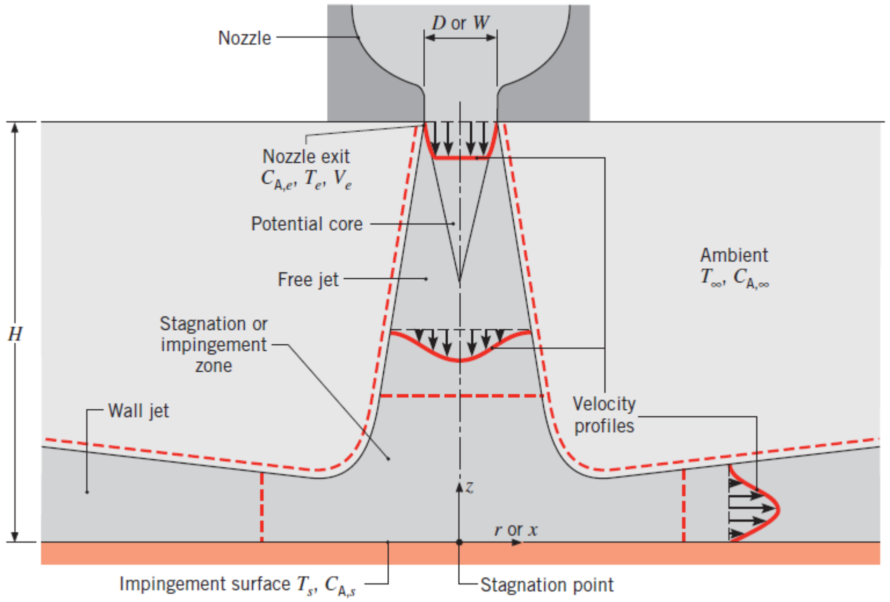

T.L. Bergman, A.S. Lavine, F.P. Incropera, Fundamentals of Heat and Mass Transfer, 7th Edition, John Wiley & Sons, Incorporated, 2011, ISBN: 9781118137253

Impinging jets are commonly used to achieve enhanced coefficients for convective heating, cooling, or drying

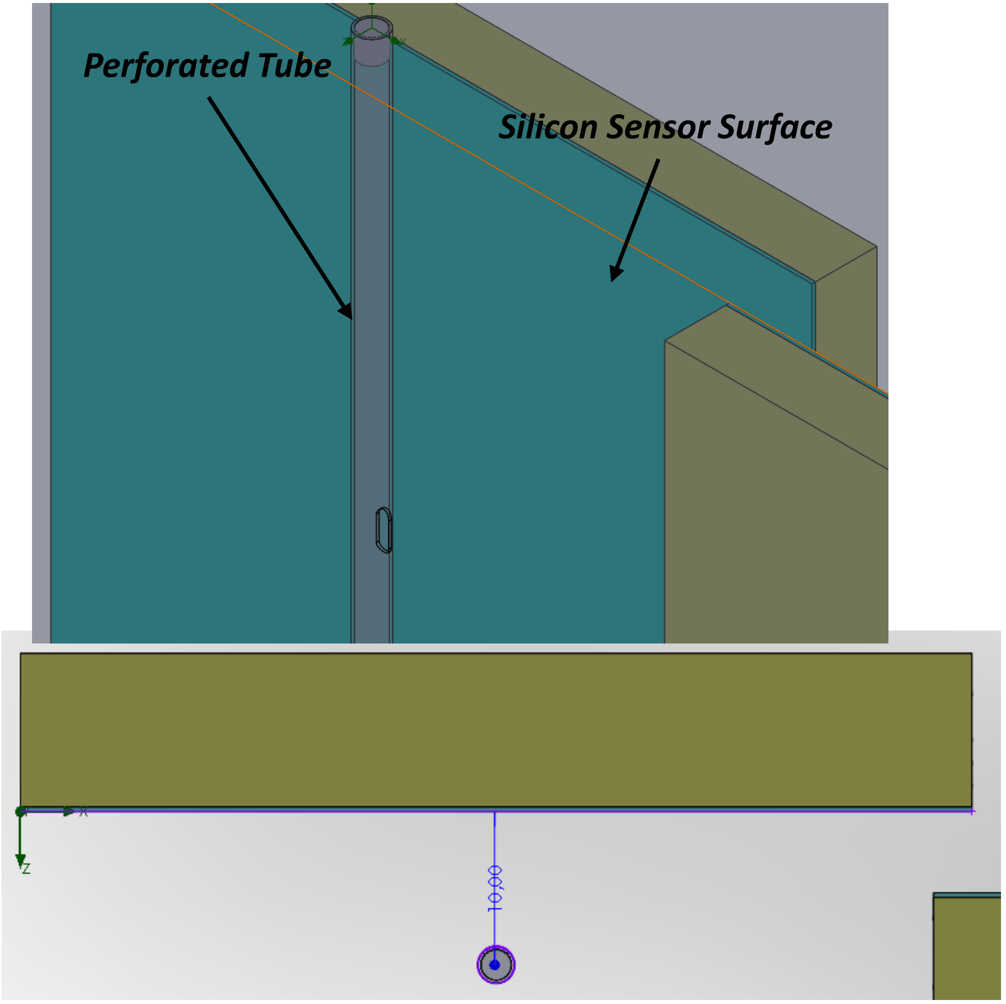

STS Front-End Electronics Cooling

Requirements On Electronics Cooling

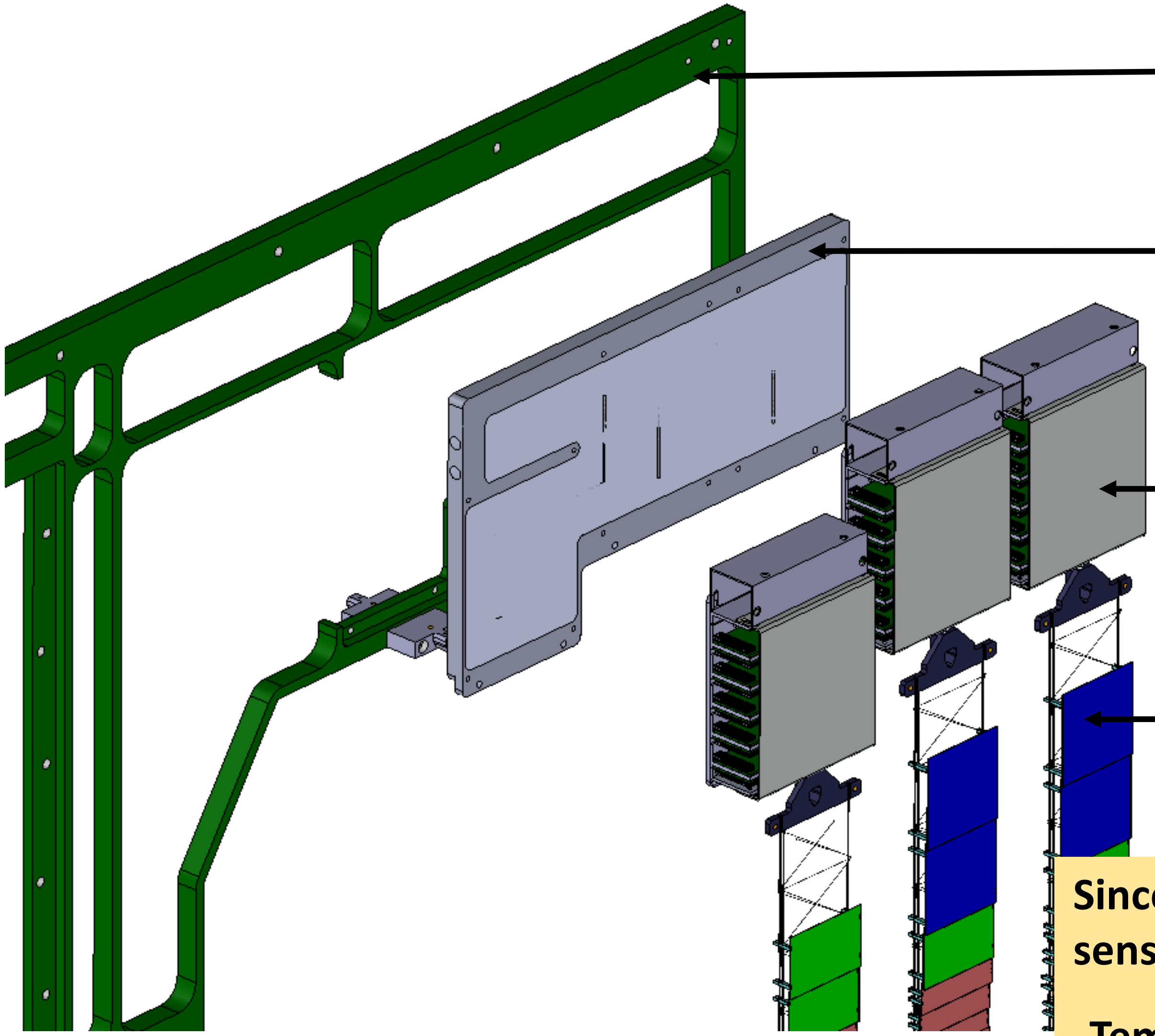

C-Frame (support structure)

Cooling Plate carrying the coolant

Front-End Electronics Board (FEB) Boxes

P_{FEB} = 10 W (approx.)

$P_{FEB\ Box}$ = 100 W

Silicon Sensor mounted on the CF ladder (microcables hidden)

Since the electronics are 25…50 cm away from the innermost sensors, one must neutralise the electronics power dissipation

Temp. exposed by the FEB Boxes ≈ Temp. on the sensors ≈ -10°C

Transition From Bi-Phase CO_2 To Mono-Phase 3M Novec 649

58 μm, strip lengths between 20 and 60 mm, and a thickness of 300 μm of silicon. According to the CBM running scenario the maximum non-ionizing dose for the sensors closest to the beam line does not exceed 1×10^{14} n_{eq} cm^{-2}. The STS is operated in a thermal enclosure that keeps the sensors at a temperature of about -5° C. The heat dissipated in the read-out electronics is removed by a CO_2 cooling system. The mechanical structure of the detector system including

J.M. Heuser (eds.) *et al.*, *Technical Design Report for the CBM Silicon Tracking System (STS)* – GSI Report 2013-4 (2013)

Biphase CO_2 (GWP = 1)

- ✓ Operational in various trackers at (HL-)LHC, ISS
- ✓ Great performance
  - less mass flow; H = 150 kJ/kg (at -20°C)
  - low pressure drop; ν = 0.14 cSt (at -23°C)
  - smaller tubes; h_{vol} = 10 kW/m².K
  - uniform temperature
- ✗ Higher system pressures i.e., safety regulations
- ✗ Potentially difficult for commercial manufacturing (2PACL-type system)

CBM-STS FEE Cooling Conceptual Design Review, 10.12.2019 | Link

Monophase 3M NOVEC 649 (GWP = 1)

- ✓ To be used in LHCb Sci-Fi Tracker. Considered for more...
- ✗ Relatively lower performance
  - higher mass flow; c_p = 1.1 kJ/kg.K
  - higher pressure drop; ν = 0.70 cSt (at -40°C)
  - larger tubes; h_{vol} = 2 kW/m².K
  - non-uniform temperature
- ✓ Lower system pressures i.e., safe to use

Based on recommendations from CERN, CBM and industrial experts, the coolant for STS-FEE is NOVEC 649

HEAT SOURCES

Heat Sources	Power Dissipation [kW]
Front End Electronics (FEE)	24.2
Readout Boards (ROBs)	4.7
Power Boards (POBs)	18.1
Heat transfer through thermal enclosure	4
Low Voltage (LV) Cables	3
Total Power Dissipation [kW]	54

Table 2: Breakdown of major power dissipation contributions by their sources. These are approximate values only which represent the worst case scenario and are dependent on the specific setting at which the electronics are operated (e.g. value of charge-sensitive-amplifier, efficiency of the DC-DC converters, etc) [9].

CFD Simulations – Cooling Plate

Cool Tec Electronic GmbH

CBM

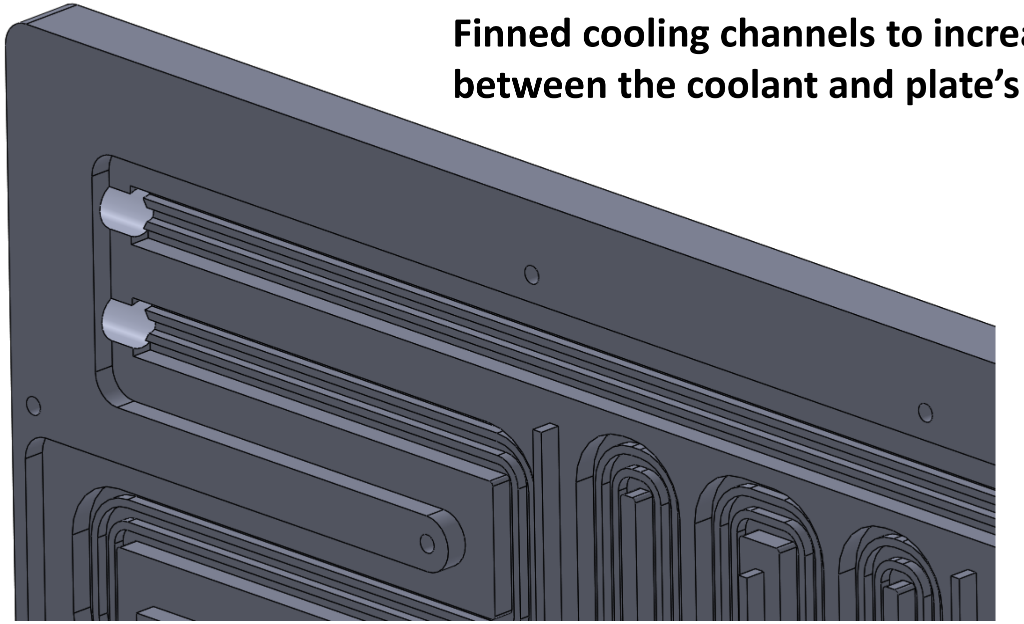

Finned cooling channels to increase heat transfer between the coolant and plate's inner surface

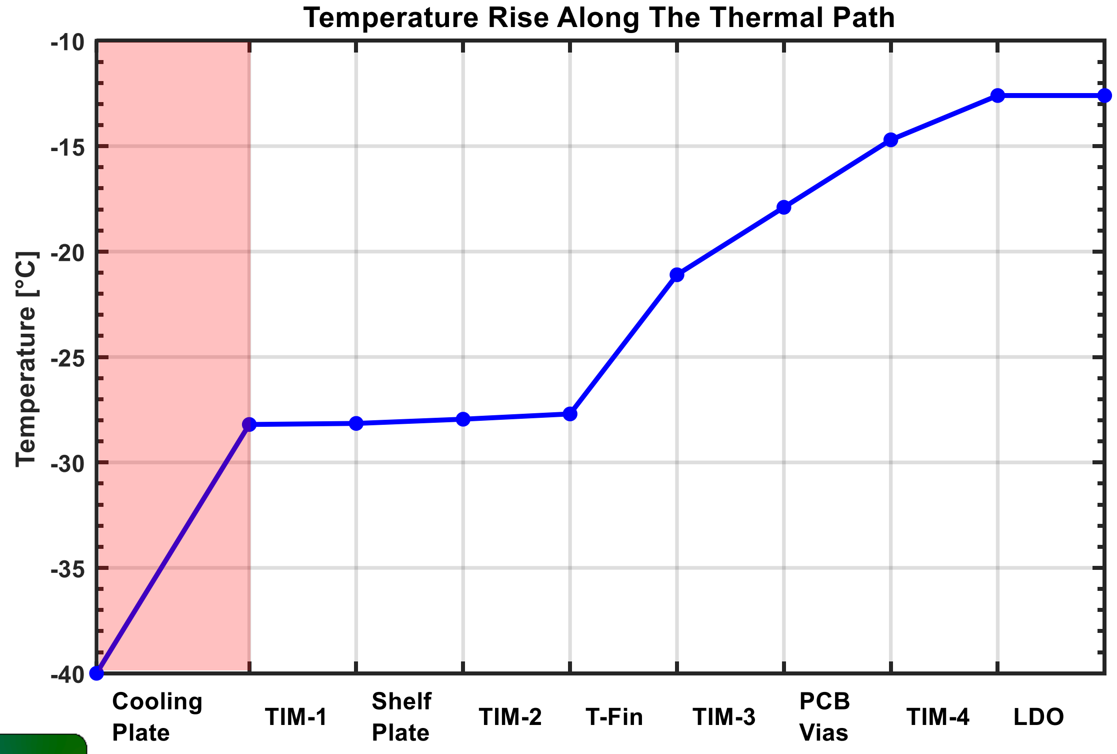

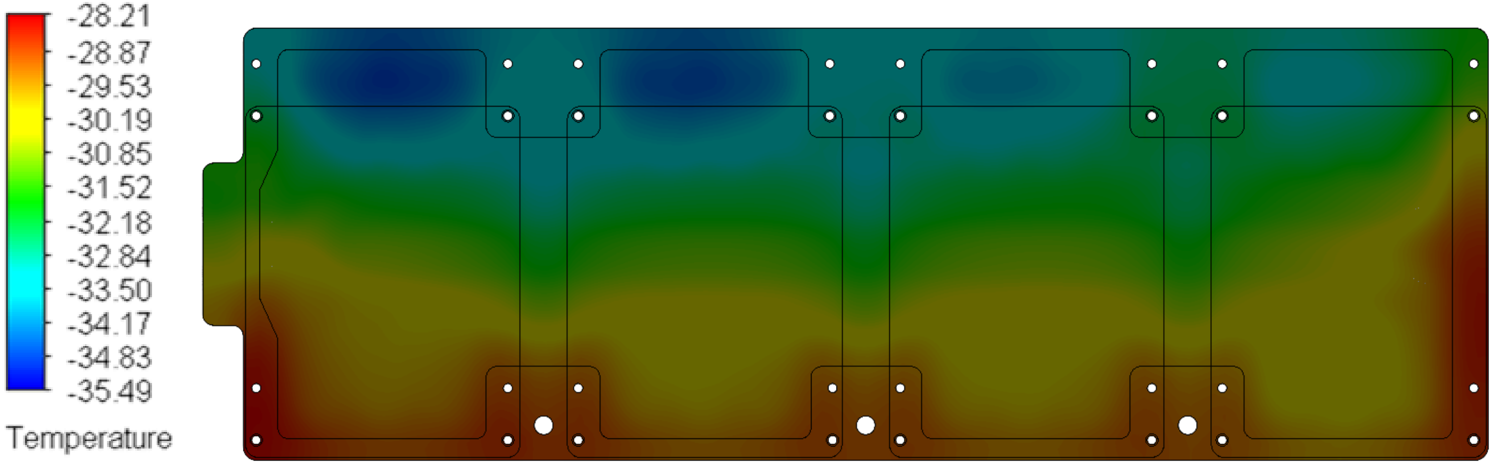

Material:	**Aluminium**
Inlet:	**3M Novec 649**
	-40°C at 3 litre/min
Total power dissipation:	**800 W**
Temperature outlet:	**-33.8 °C**
Max. temp. of cooling plate:	**-28.2 °C**
Pressure loss:	**1.32 bar**

Thermal FEA Simulations – FEB Box

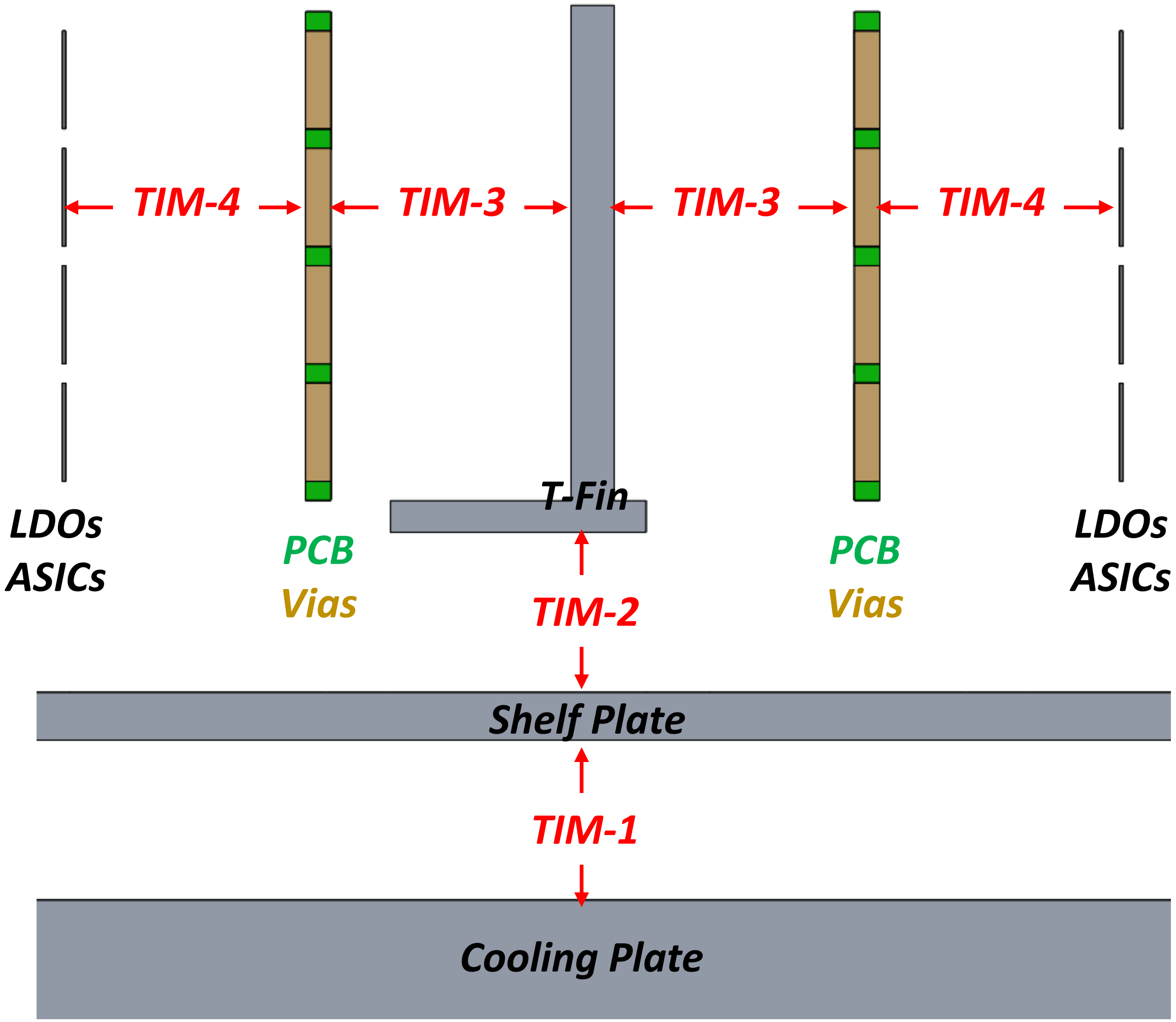

TIM: Thermal Interface Material

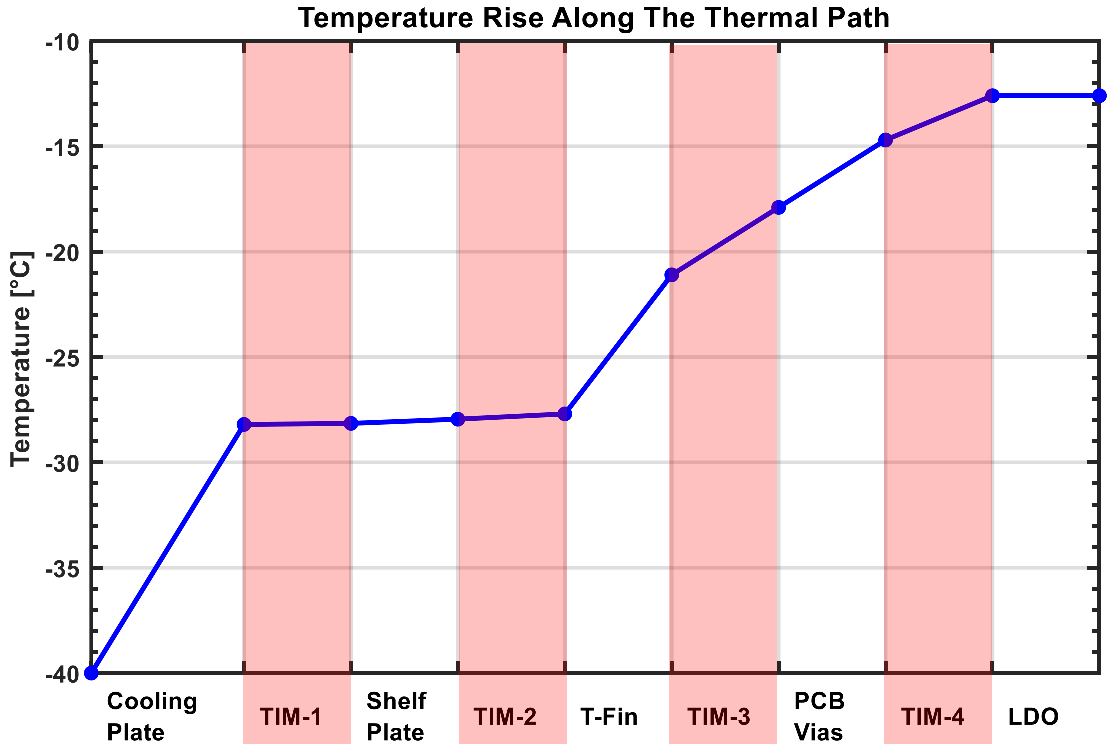

	Product	Thermal Conductivity (along z-) [W/m.K]	Thickness [µm]
TIM-1	DSN5040-10DC10DC	20	40
TIM-2	DSN5040-10DC10DC	20	40
TIM-3	Stycast 2850FT (+23LV)	1.02	150
TIM-4	EPO-TEK E4110	1.37	100

THERMAL FEA SIMULATIONS – FEB BOX

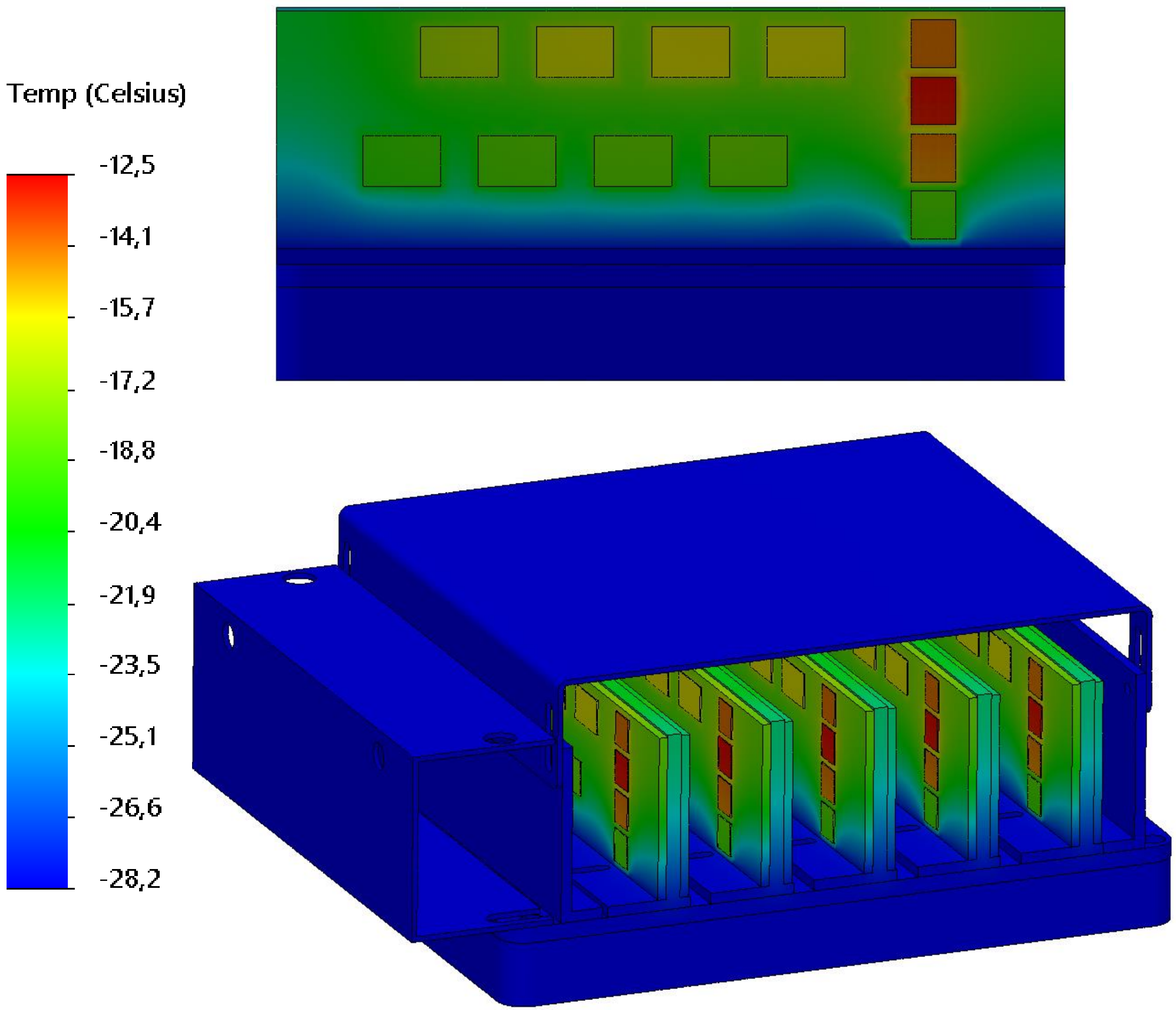

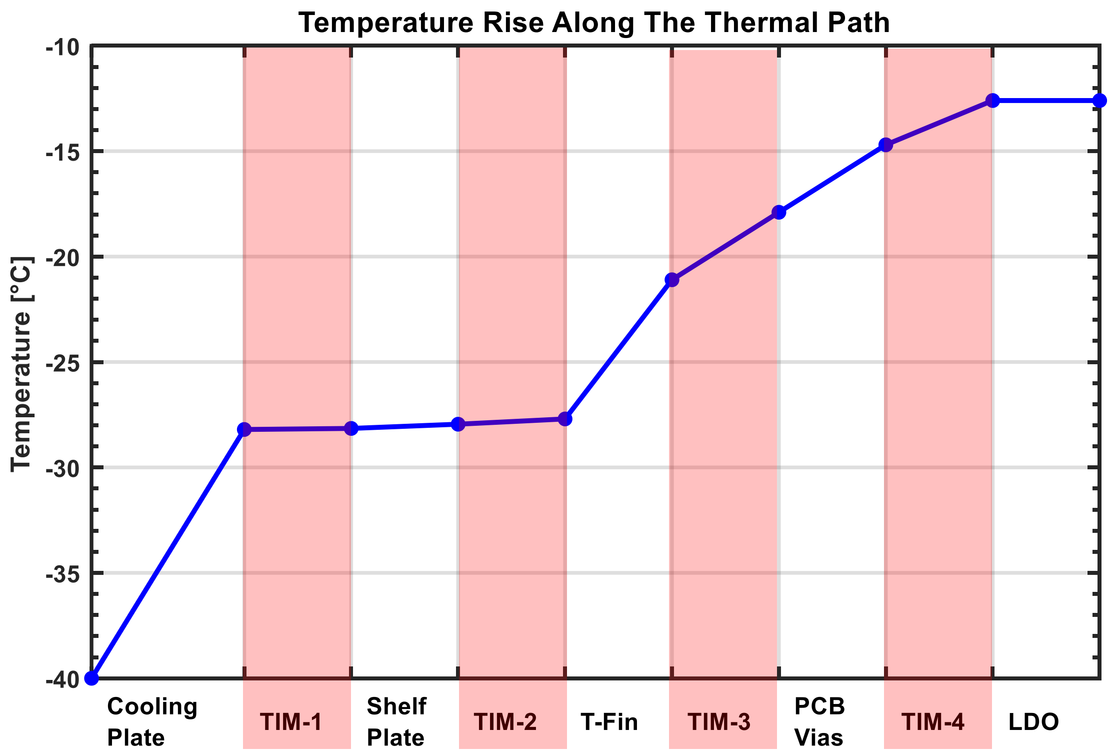

Since the temp. exposed to the environment (i.e., temp. 'seen' by the silicon sensors) is ~ -20°C which is much lower than -10°C, there is substantial headroom for increasing the coolant temp. from -40°C

Baby Cooling Plant – Simplified P&ID

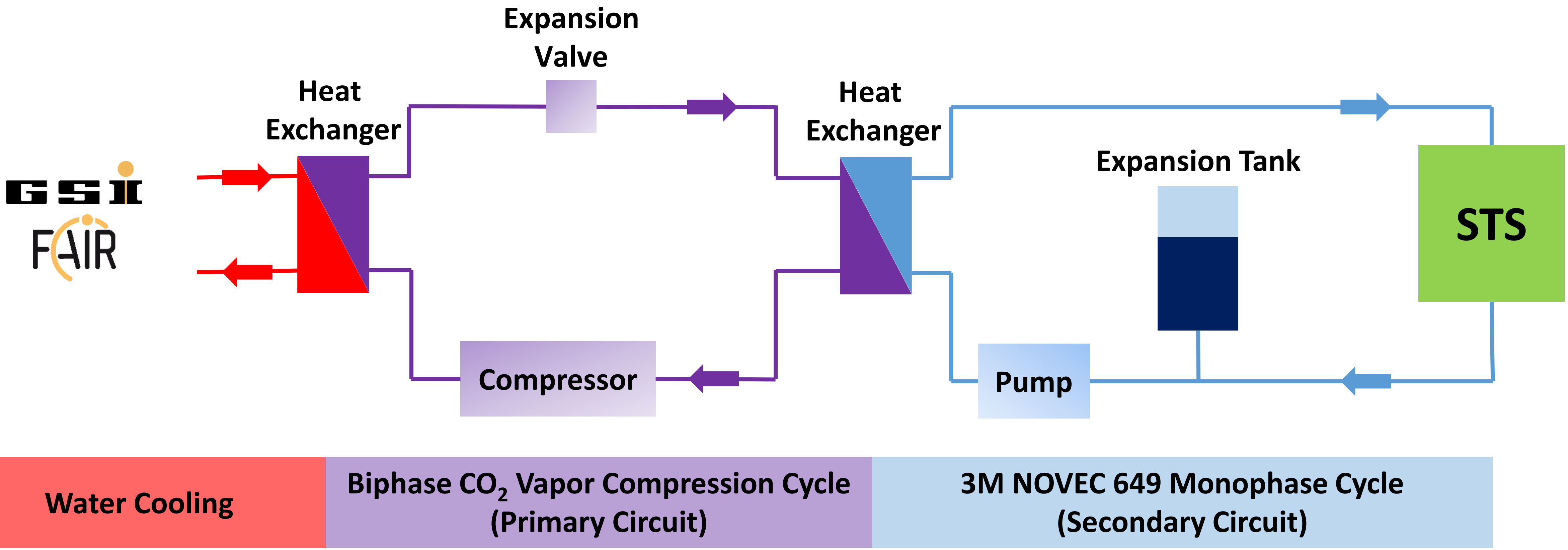

- All coolants used in this concept are GWP = 1, which makes this cooling plant usable for coming decades
- 'Simple' to manufacture commercially by using established technology and industrial practices
- To be used by STS for the Thermal Demonstrator and detector assembly procedure & testing

Biphase CO_2 Vapor Compression Cycle

3M NOVEC 649 Monophase Cycle

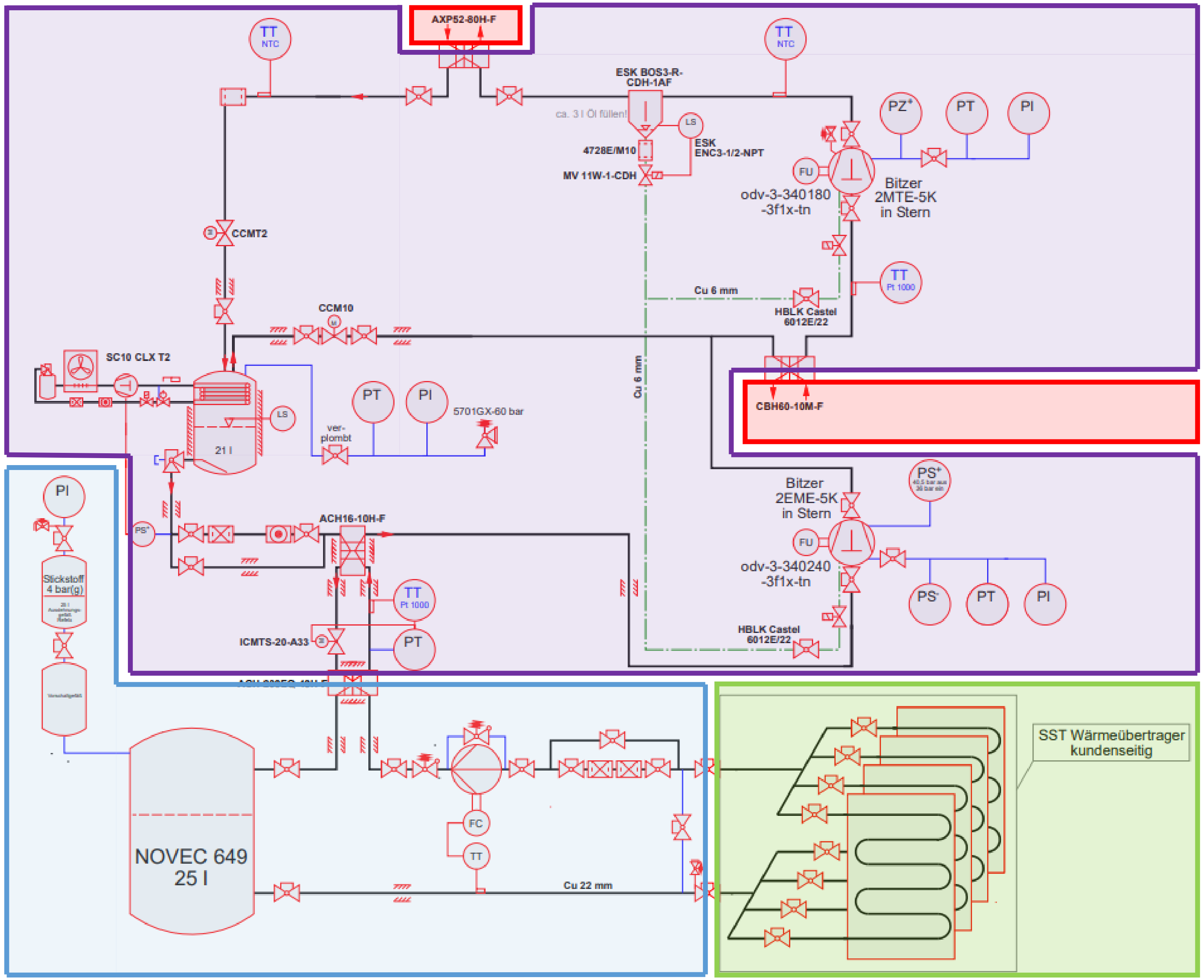

Water Cooling

STS

modeling methods are described in [17, 18]. Correlations from Martin [19] [5] are considered here as they are widely used to determine the Nusselt number (Nu) and consequently, the convective heat transfer coefficient for impinging gas jets for a range of geometrical features (see Fig. 11) and flow rates (in terms of Reynolds Number (Re), which are described below in Eq. 2.4, 2.5:

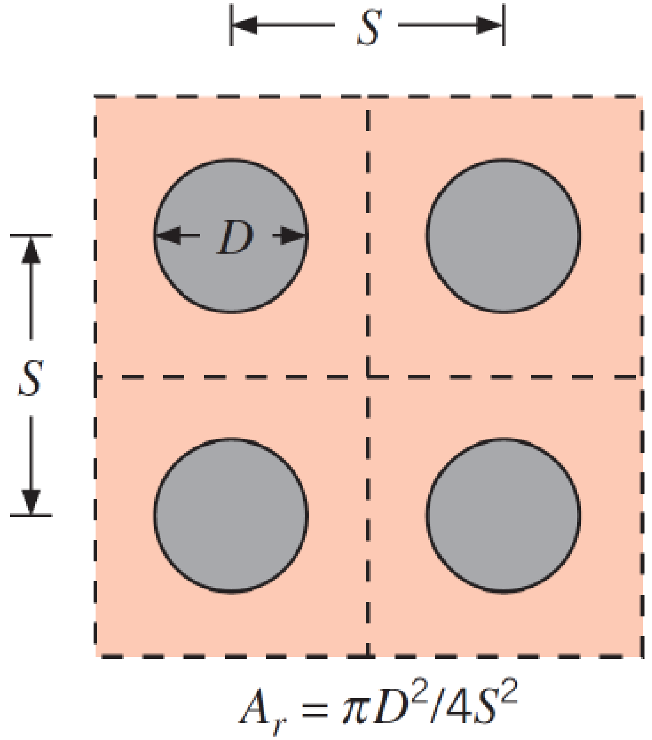

Figure 11: Plan view of an in-line array of round jets [21].

$$Nu = 0.5K\left(A_r\frac{H}{D}\right)G\left(A_r\frac{H}{D}\right)Re^{2/3}Pr^{0.42} \quad (2.4)$$

where,

$$K = \left[1 + \left(\frac{H/D}{0.6/A_r^{1/2}}\right)^6\right]^{-0.05} \quad (2.5a)$$

$$G = 2A_r^{1/2}\frac{1 - 2.2A_r^{1/2}}{1 + 0.2(H/D - 6)A_r^{1/2}} \quad (2.5b)$$

and the valid within the following range

$$\begin{bmatrix} 2000 \leqslant Re \leqslant 400,000 \\ 2 \leqslant H/D \leqslant 12 \\ 0.004 \leqslant A_r \leqslant 0.04 \\ 4 \leqslant S \leqslant 14 \end{bmatrix}$$

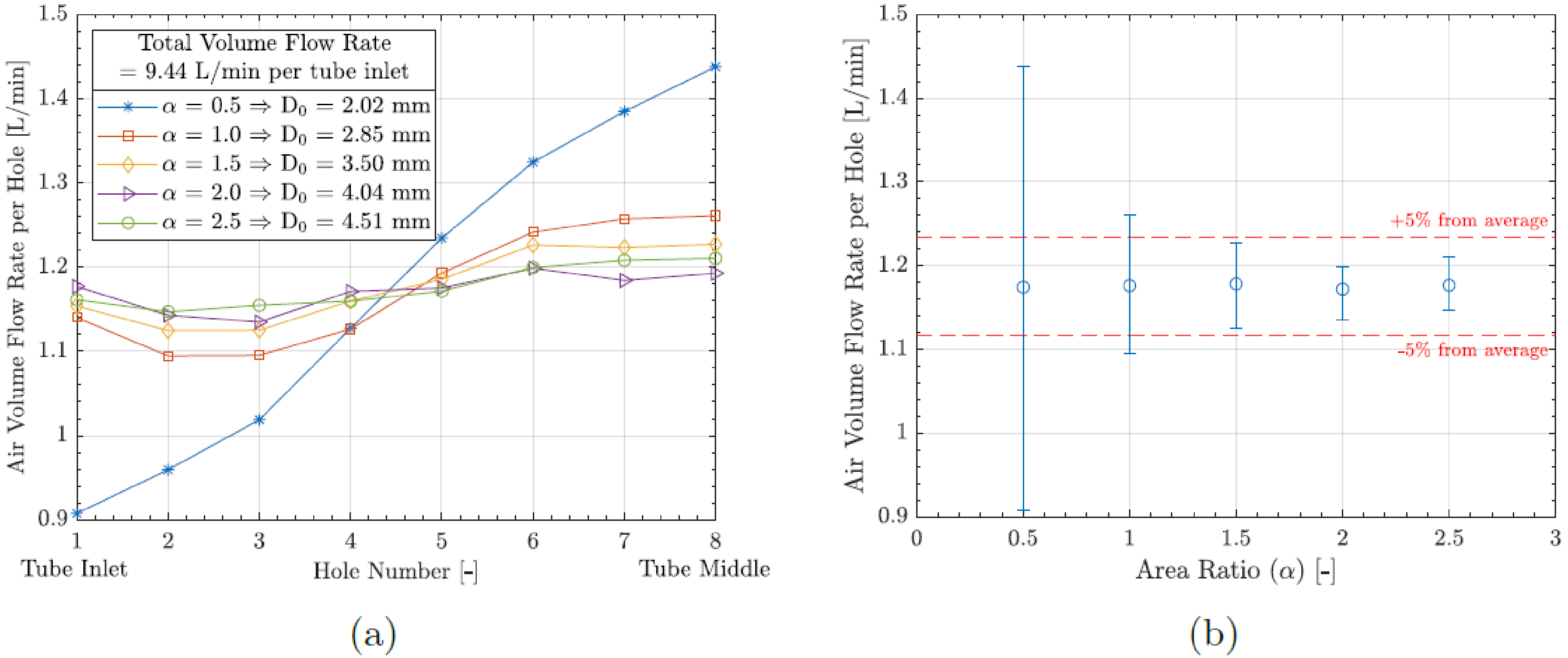

Figure 13: (a) Variation of the volumetric air flow rate [L/min] from each hole for various tube diameters (D_0) or area ratios (α). The plot is only for half of the tube's actual length because the air flow is expected to be symmetric when air inlet is from both ends of the tube. (b) The same plot as shown in the left. This shows the deviation of flow rate per hole from the average flow rate, where the error bars show the extent of flow deviation from the left plot.

Inner Diameter (D_0)	3.50 mm
Shell Thickness	0.25 mm
Material Budget (local)	0.68% x/X_0
Material Budget (averaged over sensor area)	0.02% x/X_0
Pitch (S)	14 mm
Length (L) per half	100 mm
Number of Holes (N) per half	8
Height (H) from the innermost sensor of a normal (central) ladder	12 mm (10.5 mm)

Table 3: Properties of the carbon-fibre based perforated tube. Since gas flow will enter from both sides of the tube, values for tube length and number of holes are quoted for half of the tube's actual length.